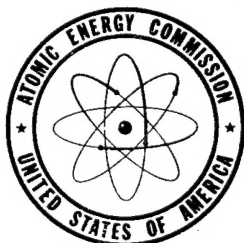# UNITED STATES ATOMIC ENERGY COMMISSION

AECD-3237

THE CRYSTAL STRUCTURES OF SOME THORIUM AND URANIUM COMPOUNDS

By
Norman Charles Baenziger

October 15, 1948

Ames Laboratory

Technical Information Service, Oak Ridge, Tennessee

DTIC QUALITY INSPECTED 3

19961216 149

CHEMISTRY

TABLE OF CONTENTS

4

THE CRYSTAL STRUCTURES OF SOME THORIUM AND URANIUM COMPOUNDS[1]

by

Norman Charles Baenziger

ABSTRACT

The Structure of the U_6M Compounds

Isostructural compounds with the composition U_6M (where M = Mn, Fe, Co, and Ni) have been found and the structure determined. Single crystals, examined by the rotation, oscillation, Laue, and Weissenberg methods, exhibited the diffraction symmetry D_{4h} - 4/mmm. The unit cell dimensions of the body-centered tetragonal compounds are for U_6Mn, $a = 10.29$ A₀, $c = 5.24$ A₀; for U_6Fe, $a = 10.31$ A₀, $c = 5.24$ A₀; for U_6Co, $a = 10.36$ A₀, $c = 5.21$ A₀; and for U_6Ni, $a = 10.37$ A₀, $c = 5.21$ A₀. There are four U_6M in a unit cell.

The general absences which were observed other than those due to body-centering are $(0k\ell)$ with k odd and ℓ odd. Since all the space groups which satisfy these intensity requirements and possess appropriate positions for the atoms have the same structure factor for $(hk0)$ reflections, the approximate positions for the uranium atoms were found by plotting the F values for the very strong reflections and for the absent reflections. These positions were further refined by the Fourier method using the $(hk0)$ data. The z parameters were chosen by examination of the (00ℓ) data, but because of the effect of absorption on the intensities, the determination of the z parameter is uncertain. The final uranium positions are described by space group D_{4h}^{18} with

(add $000, \frac{111}{222}$ to all positions)

16 U at $xy0$; $\bar{x}\bar{y}0$; $\bar{y}x0$; $y\bar{x}0$; $\bar{x}y\frac{1}{2}$, $x\bar{y}\frac{1}{2}$; $yx\frac{1}{2}$; $\bar{y}\bar{x}\frac{1}{2}$;
     with $x = 0.2141$, $y = 0.1021$,

8 U at $x, \frac{1}{2} + x, 0$; $\bar{x}, \frac{1}{2} - x, 0$; $\frac{1}{2} + x, \bar{x}, 0$; $\frac{1}{2} - x, x, 0$;

4 M at $00\frac{1}{4}$; $003/4$.

The possible variations of the z parameter are permitted in D_4^9 and D_{2d}^{10}.

The application of Pauling's valence and radii rules led to valences of ~ 5.4 for uranium and 4.5 for the transition metal atom. The zone bounded by the planes due to (600) and (002) contains the proper number of electrons if Hume-Rothery's valences are used. This is probably not very significant, however.

The Structure of the Th_7M_3 Compounds

The Th_7M_3 compounds (where $M = Fe$, Co, and Ni) crystallize with a hexagonal unit cell whose dimensions are for Th_7Fe_3, $a = 9.85$ A.; $c = 6.15$ A.; for Th_7Co_3, $a = 9.83$ A., $c = 6.17$ A.; and for Th_7Ni_3, $a = 9.86$ A., $c = 6.23$ A. There are two Th_7M_3 in a unit cell. Single crystals, examined by rotation and Weissenberg methods, exhibited the diffraction symmetry of D_{6h}.

The approximate (x,y) positions of the thorium atoms were determined from a Patterson projection of the (hk0) data. These positions were further refined by the Fourier method. The positions of the iron atoms were never clearly resolved and were determined mostly from spatial considerations. The determination of the z parameter was again subject to absorption errors. From the intensity data it was clear, however, that the atoms were arranged in four layers, each approximately one-fourth of c apart. The final z parameters chosen are those which yield reasonable interatomic distances as well as satisfy the intensity data. These positions are found in space group C_{6v}^4 with

2 Th at $1/3, 2/3, z$; $2/3, 1/3, 1/2 + z$; with $z = 0.06$

6 Th at $x, 2x, z$; $2\bar{x}, \bar{x}, z$; $x, \bar{x}, z$; $\bar{x}, x, \frac{1}{2} + z$; $\bar{x}, 2\bar{x}, \frac{1}{2} + z$;

$2x, x, \frac{1}{2} + z$; with $x = 0.126$ and $z = 0.250$,

6 Th at the same positions with $x = 0.544$ and $z = 0.03$,

6 M at the same positions with $x = 0.815$ and $z = 0.31$.

Pauling's radii give the thorium atoms valences of approximately four and the transition metal atom ~ 4.5. Again, a zone may be found which will contain the number of electrons expected using Pauling's valences. It is not clear, however, that this is the factor which determines the stability of the structure.

The Structures of U_2O_5 and U_3O_8

The uranium oxides other than UO_2 have been investigated previously and the existence of a one phase region extending from $UO_{2.62}$ to UO_3 has been reported, but only recently have structures been proposed for the oxides U_3O_8 and UO_3. Single crystals of the oxide, U_2O_5, which forms the lower limit of the one phase region have been found which have enabled a determination of its structure. Also powder diagrams of U_3O_8 have indicated the need for a larger unit cell than has been reported.

The Weissenberg diagrams of U_2O_5 showed that the crystal had the diffraction symmetry of D_{2h} - mmm. The unit cell dimensions were found to be $a = 6.73$ A., $b = 31.71$ A., $c = 8.29$ A. The pseudo cell dimensions, $a = 6.7\overline{3}$ A., $b = 3.9\overline{6}4$ A., $c = 4.1\overline{4}5$ A., corresponded to the pseudo cell dimensions of U_3O_8 already reported. Because of the relative strength of reflections at high angles, it was assumed that the weak reflections requiring the large unit cell were due primarily to uranium atoms which were slightly removed from the ideal positions occupied in the pseudo unit of UO_3.

Trial and error methods guided by Patterson projections determined approximate values of the x, y, and z parameters which were then refined by the Fourier method. Only space groups which had eight-fold positions were used. Two slightly different arrangements which gave very good agreement with the intensity data were found for the (x,y) coordinates of the atoms. The z parameters corresponding to these two arrangements are uncertain because of the absorption errors. The two possible structures are given below.

I in D_{2h}^{16}

8 U at xyz; $\overline{x}\overline{y}\overline{z}$; $\overline{x},\overline{y},\frac{1}{2}+z$; $x,y,\frac{1}{2}-z$; $\frac{1}{2}+x,\frac{1}{2}-y,\overline{z}$; $\frac{1}{2}+x,\frac{1}{2}-y,\frac{1}{2}+z$; $\frac{1}{2}-x,\frac{1}{2}+y,\frac{1}{2}-z$; $\frac{1}{2}-x,\frac{1}{2}+y,z$; with $x = 0.2825$, $y = 0.0352$, $z = 0.013$,

8 U in the same positions with $x = 0.745$, $y = 0.092$, $z = 0.993$,

8 U in the same positions with $x = 0.2067$, $y = 0.1546$, $z = 0.995$,

8 U in the same positions with $x = 0.745$, $y = 0.2227$, $z = 0.016$.

II in D_{2h}^{5}

8 U at xyz; $\overline{x}\overline{y}\overline{z}$; $xy\overline{z}$; $\overline{x}\overline{y}z$; $x,\frac{1}{2}-y,z$; $\overline{x},\frac{1}{2}+y,\overline{z}$; $x,\frac{1}{2}-y,\overline{z}$; $\overline{x},\frac{1}{2}+y,z$; with $x = 0.539$, $y = 0.0591$, $z = 0.259$,

8 U in the same positions with $x = 0.988$, $y = 0.1295$, $z = 0.244$,

8 U in the same positions with $x = 0.505$, $y = 0.1841$, $z = 0.238$,

4 U at $x\frac{1}{4}z$; $x\frac{1}{4}\bar{z}$; $\bar{x},3/4,z$; $\bar{x},3/4,\bar{z}$; with $x = 0.047$ and $z = 0.265$,

4 U at $00z$, $00\bar{z}$; $0\frac{1}{2}z$; $0\frac{1}{2}\bar{z}$; with $z = 0.220$.

If a unit cell of the same dimensions as U_2O_5 is chosen in the UO_3 structure, then only the symmetry of C_{2h} or lower is possible. Although the uranium positions may be described by orthorhombic space groups, the oxygen positions must be described by monoclinic space groups. If only a slight change has taken place, the oxygen atom positions in U_2O_5 may also be described by monoclinic space groups. Space group C_{2h}^5 describes the uranium positions as in D_{2h}^5 (with suitable parameters) and allows the oxygen positions to be varied from their positions in UO_3.

The unit cell of U_3O_8 is made up of three orthorhombic cells of UO_3 (less two oxygen atoms) stacked in the b direction. All the reflections which were observed were of the type $(hk0)$ with $h + k$ equal to $2n$. The intensity data indicated the presence of both an $\bar{x}$ and y parameter for the uranium positions, hence, only space group C_{2v}^{14} has the required positions. The uranium atoms were found to be in the following positions:

(add 000, $\frac{1}{2}\frac{1}{2}0$ to all positions)

2 U at $x00$ with $x = 0$,

4 U at $xy0$; $xy0$; with $x = 0.04$ and $y = 0.326$.

Rotation diagrams of U_2O_5 normal to (130) indicated an approximate tripling of the pseudo cell axis which might correspond to U_3O_8 (actually instead of weak first and second layer lines and a strong third layer line, the layer lines, 1, 5, 6, 10, 11, 15, 17, etc. were weak and 16 and 32 strong). This might indicate that the cells were chosen at a rotation of approximately 60°.

The location of missing oxygen atoms from the UO_3 arrangement in U_2O_5 and U_3O_8 is difficult. Some of the uranyl oxygens are undoubtedly gone, however. The number of additional vacancies cannot be decided further.

A New Method for Determining X-ray Intensities

A new method for determining the intensities of X-ray reflections from the record on photographic film has been developed which involves

the radioactive toning of the film. Upon considering the various toning
and intensifying processes and the isotopes now available, the cobalt-
ferricyanide toning process seemed to be most promising. An investiga-
tion of the toning conditions disclosed that the two step process, using
a ferricyanide bleach (5% $K_3Fe(CN)_6$ plus 10 drops of NH_4OH per 100 ml.
of water) and a radioactive toner of cobalt bromide (0.04 g. Co in 100
ml. water, 1.2 millicuries of activity) was suitable. The films, con-
ventionally developed, fixed, washed, and dried, are soaked thirty min-
utes in water, placed in the bleach for at least thirty minutes, washed
in running water for an hour, toned in $CoBr_2$ for at least thirty minutes,
placed in several beakers of water for several hours to dilute the
occluded and absorbed activity, washed in running water, and dried. The
spots are punched from the film base and counted using a Victoreen Gei-
ger-Müller counter.

The method has been tested on anthracene crystals and has been
found to give results accurate to approximately 5 per cent. The inten-
sity of a spot can be determined in two to ten minutes time depending
on the size of the spot and its intensity.

INTRODUCTION

The chemistry and metallurgy of thorium and uranium were investi-
gated extensively by workers on the Manhattan Project during the past
few years. These investigations were pursued by all available scientific
methods. Among these, the X-ray diffraction method provided a powerful
tool for phase identification and structure determination, which greatly
assisted in the solution of the metallurgical and chemical problems.

Intermetallic Compounds

Although the application of the X-ray diffraction method to the
study of the binary systems of uranium with other metals was originally
intended to supplement the thermal and microscopic investigations, the
structural investigations which resulted had additional value in rela-
tion to the theory of metals. Several attempts have been made to ex-
plain or to correlate the compounds which are formed between metals.
Each of these suggestions have been partially successful when applied to
select groups of compounds, and totally unsuccessful when applied to
others. All methods involve some assumption with regard to the valence

of the metal atoms. Since the valence of the transition metals has
been assumed to be constant in several of these hypotheses, and since
the size of the metal atoms does not vary markedly, the series of in-
termetallic compounds formed by uranium and thorium with these elements
are quite interesting.

It was observed in the uranium series that the number of inter-
metallic compound phases increased from chromium, where none existed,
to nickel, where four compounds existed; the number of compounds was
again less in the copper and zinc systems. The investigation of the
thorium systems, by X-ray methods alone, were begun to determine if
any similarity existed between the thorium and uranium systems. Again,
it was found that the number of compounds increased from the chromium
system, which had none, to the thorium-nickel system. The thorium-
copper system apparently does not parallel the uranium system, however,
as it appears to be fairly complex. A structural relationship between
corresponding thorium and uranium compounds does not appear to exist,
however, since all the known uranium compounds crystallize with tetra-
gonal or cubic unit cells and all the known thorium compound phases
occur with hexagonal unit cells.

Most of the intermetallic compounds in the uranium and thorium
systems were isostructural with other alloy phases already known. Two
new structure types, U_6M and Th_7M_3, were found, however, and it is the
structural determination of these compounds which is reported in the
second and third parts of this thesis.

Uranium Oxides

The oxides of any element have always been important compounds
since they are the product of the reaction of the element with the most
active component of the atmosphere. The uranium oxides, especially the
higher oxides, are particularly interesting since inorganic chemists
have long endeavored to understand U_3O_8 and have conjectured concerning
the existence of U_2O_5. Also, it has been known from vapor pressure data
and from preliminary X-ray diffraction studies that a one phase region
apparently exists from UO_3 extending to some lower uranium oxygen ratio.
Thus, the relationship of the structures of U_3O_8 and the lower limit of
the one phase region to UO_3 present interesting structural problems
which would greatly clarify the picture of the uranium-oxygen system.
A structural investigation of these problems is presented in the fourth
part of the thesis.

Method of Determining X-ray Intensities

In the course of the structural investigations mentioned above, it was found that the measurements of the X-ray intensities were unsatisfactory. Although many methods of measuring X-ray intensities have been devised since the discovery of X-rays in 1895, the most common methods rely on the darkening of photographic film and the ionization of gases by X-rays. Some of the methods which have been devised are suitable only for specific problems. The specific problem of the measurement of the intensities of the reflections from single crystals has been attacked by many investigators. No method has been developed, however, which has proved wholly satisfactory. Measurements which are the most accurate and convenient require very special equipment. The new method of determining intensities, presented in the last part of this thesis, involves the radioactive toning of the photographic record of the diffraction pattern. This method requires only standard counting tubes and circuits used in radioactive studies in chemistry and physics. This equipment is now becoming available in a large number of modern laboratories as standard equipment.

THE STRUCTURE OF THE U_6M COMPOUNDS

Introduction

Metallurgical studies of the uranium-transition metal systems have been undertaken at several different laboratories. The uranium-iron system was investigated by Kaufmann et al. (1), who reported Bragg spacings for U_6Fe and the unit cell of UFe_2. The uranium-nickel system was studied by Foote et al. (2). They reported the existence of the compounds U_6Ni, UNi, UNi_2, and UNi_5. The X-ray data which they reported, however, were completely erroneous. The thermal and microscopic studies of the uranium-manganese and the uranium-cobalt systems were performed by Carlson and Noyce (3,4), respectively. The X-ray diffraction studies of these systems were performed by Rundle et al. (5). In addition, the X-ray diffraction studies of the uranium-nickel and the uranium-iron systems were repeated, and the complete X-ray data and structures of all the intermetallic compounds with the exception of UNi were found.

The Determination of the Composition of U_6M

Preparation and occurrence of the compounds

The alloys were prepared by fusing uranium metal and the transition element in a beryllia crucible in a vacuum. After cooling, samples were prepared for powder diagrams by reducing the alloy to a fine powder in a diamond mortar and powder annealing for several hours just below the lowest transition temperature indicated by thermal studies. Occasionally, single crystals of the compound in the form of needles with a square cross-section were found in alloys of 60-80 atomic per cent uranium. These needles were separated from the rest of the alloy either mechanically or chemically (see below).

The peritectic compounds, U_6M, were found to occur in the alloy systems of uranium with manganese, iron, cobalt, and nickel. Powder diagrams of the alloys in the region of 85 atomic per cent uranium were almost identical for all four systems. The powder data obtained from U_6Fe samples agreed with those of Kaufmann (1). In addition, single crystal rotation diagrams of each of the compounds appeared identical to one another.

The composition of U_6M

The composition of U_6Fe and U_6Ni had been determined by Kaufmann (1) and Foote (2) by chemical analysis of alloys whose microstructure or X-ray diagrams appeared to indicate one phase. This composition was found to be consistent with the unit cell volume assuming the additivity of atomic volumes (6). The observed volume of the unit cell is 557 A^3, for U_6Fe; the calculated volume is 547 A^3.

A more direct approach to the determination of the composition was made possible by the discovery by Rundle (5) that dilute acids preferentially dissolved the eutectic matrix in alloys of 60-80 atomic per cent uranium leaving single crystals of the compound only slightly pitted. Large quantities of these single crystals were separated and analyzed chemically. The composition found by chemical analysis for the cobalt compound was $U_6Co_{1.09}$. (A similar result was found for the manganese compound). This result was high in cobalt, undoubtedly because the needles were separated from a cobalt rich matrix.

X-ray Diffraction Data

Experimental methods

Equipment. All of the powder diagrams were prepared in a powder camera of 5.73 cm. radius with the film mounted in the Straumanis fashion. The powdered alloy sample was contained in a sealed, thin-walled, Pyrex capillary approximately 0.2 mm. in diameter. The single crystal diagrams were prepared in a single crystal rotation camera of five centimeters radius and in a Weissenberg camera of 2.836 cm. radius. The single crystals, about 0.003 cm. in diameter, did not need to be protected from the atmosphere.

Source of X-rays. Nickel filtered copper characteristic K radiation was used for the powder and single crystal investigations. Laue diagrams were prepared using the continuous radiation from a tungsten target of a self-rectifying gas tube operated at fifty kilovolts.

Intensity determination and correction. The intensities of the (hk0) and (hkl) reflections were estimated visually from single crystal rotation diagrams by comparison with spots of known intensity on diagrams of a known structure (7). The (00l) reflections were estimated from Weissenberg diagrams by visual comparison of five multiple films.

The F_{hk0} used in the Fourier projection were determined from the intensities by the following formula,

$$\left|F_{hk0}\right| \propto \sqrt{I/LPMA},$$

where F is the structure factor; I, the observed intensity; LP, the Lorentz and polarization factors; A, the absorption factor; and M, the multiplicity factor. The absorption factor was determined by evaluating the integral $\int e^{-\mu D}\, dA$ over the cross-sectional area of the needle. μ is the linear absorption coefficient, and D is the path length of the X-rays in the crystal in scattering from the element of area, dA. The calculations were simplified because of the high absorption coefficient ($\mu = 6200$ cm.$^{-1}$) and the square cross-section of the crystal. The absorption corrections for the (hkl) planes were assumed to be the same as those for the corresponding (hk0) planes.

The calculated intensities appearing in the tables for comparison with the measured values were calculated in the following manner. The intensities I' were calculated using the formula,

$$I' \propto FF*LPAM,$$

where F* is the complex conjugate of F and the other symbols have the
same meaning as above. The Ott velocity factor is included in the
Lorentz factor for calculations of the (hkl) data. In order to correct
for the temperature factor the logarithms of $I_{obsd.}/I'$ were plotted
against $sin^2 \theta$. The straight line drawn through the points determined
the average temperature factor as a function of $sin^2 \theta$. All the inten-
sity values were then adjusted for this temperature effect.

Unit cell dimensions of the U₆M compounds

Single crystals of U_6Mn, U_6Fe, U_6Co, and U_6Ni were examined and
found to produce almost identical single crystal rotation diagrams.
The single crystal rotation diagrams were indexed by using a body-
centered tetragonal lattice obtained by Wilson and Rundle (5). The unit
cell dimensions which are listed in table 1 were determined from powder
diagrams. The X-ray densities, $\mathcal{C}$, are reported on the basis of four
units of U_6M per unit cell.

Table 1

Unit Cell Dimensions of the U_6M Compounds[a]
(in Angstroms)

	a	c	$\mathcal{C}$ in gm/cc
U₆Mn	10.29 ± .01	5.24 ± .02	17.8
U₆Fe	10.31 ± .04	5.24 ± .02	17.7
U₆Co	10.36 ± .02	5.21 ± .02	17.7
U₆Ni	10.37 ± .04	5.21 ± .02	17.6

[a]The dimensions are expressed in true Angstrom units (8).

Determination of the Laue symmetry

Oscillation and Weissenberg diagrams were taken with the axis of
rotation along the a and along the c axes of the crystal. Laue diagrams

were taken v h the X-ray beam normal to and along the c axis of the crystal. All these methods indicated mirror planes both perpendicular to the four-fold axis and containing the four-fold axis. The Laue symmetry is, then, $D_{4h} - 4/mmm$.

<center>Structural Determination</center>

Space group determination

All the reflections which were observed can be classified in the following manner.

$(hk\ell)$	present only with $\underline{h} + \underline{k} + \underline{l}$ even,
$(hk\mathit{0})$	present only with $\underline{h} + \underline{k}$ even,
$(\overline{0k\ell})$	present only with $\underline{k}$ even and $\underline{\ell}$ even,
$(hh\ell)$	present only with $\underline{\ell}$ even.

The $(hk\ell)$ data require a body-centered unit-cell. The $(hk0)$ data require that there are neither "a" nor "b" glide planes perpendicular to the c axis. The $(0k\ell)$ data indicate that there is an "a" glide plane perpendicular to the b axis, a "b" glide plane perpendicular to the a axis, a "c" glide plane perpendicular to the a or b axes, or an "n" glide plane present. The $(hh\ell)$ data indicate the absence of a $(1\overline{1}0)$ glide plane with a "d" glide. The characteristic extinctions due to two-fold screw axes are masked by the requirements of a body-centered lattice. There are no indications of a 4_1 or a 4_3 screw axis.

Space groups which do not permit twenty-four uranium atoms and four transition metal atoms in the unit cell do not need to be considered. Therefore, only the space groups listed in table 2, which satisfy the symmetry requirements, are possible. The twenty-four uranium atoms may be in a sixteen-fold set of equivalent positions plus an eight-fold set of equivalent positions, in three eight-fold sets of positions, or in a larger number of more special sets of positions. The sixteen and eight-fold sets will be considered first.

The sets of positions which place uranium atoms directly above one another along the c axis place uranium atoms only 2.61 A. apart. Since the closest uranium-uranium distance in uranium metal is 2.76 A., it will be assumed that these positions are unsuitable. The sixteen- and eight-fold sets of equivalent positions which are not eliminated by this assumption are given in table 2.

Table 2

Possible U Atom Positions in the U_6M Structure

Space group		Positions (Add $000, \frac{1}{2}\frac{1}{2}\frac{1}{2}$ to all positions)
D_{4h}^{18}	16 (k)	$xy0$; $\overline{xy}0$; $\overline{y}x0$; $y\overline{x}0$; $x\overline{y}\frac{1}{2}$; $\overline{x}y\frac{1}{2}$; $yx\frac{1}{2}$; $\overline{y}\overline{x}\frac{1}{2}$;
	8 (h)	$x,\frac{1}{2}+x,0$; $\overline{x},\frac{1}{2}-x,0$; $\frac{1}{2}+x,\overline{x},0$; $\frac{1}{2}-x,x,0$;
D_{4h}^{17}	16 (l)	$xy0$; $\overline{xy}0$; $\overline{y}x0$; $y\overline{x}0$; $x\overline{y}0$; $\overline{x}y0$; $yx0$; $\overline{y}\overline{x}0$;
	8 (h)	$xx0$; $\overline{x}\overline{x}0$; $x\overline{x}0$; $\overline{x}x0$;
	8 (i)	$x00$; $\overline{x}00$; $0x0$; $0\overline{x}0$;
	8 (j)	$x\frac{1}{2}0$; $\overline{x}\frac{1}{2}0$; $\frac{1}{2}x0$; $\frac{1}{2}\overline{x}0$;
D_4^9	16 (k)	xyz; $\overline{xy}z$; $\overline{x}y\overline{z}$; $x\overline{y}\overline{z}$; $yx\overline{z}$; $\overline{y}\overline{x}\overline{z}$; $\overline{y}xz$; $y\overline{x}z$;
	8 (g)	$xx0$; $\overline{x}\overline{x}0$; $x\overline{x}0$; $\overline{x}x0$;
	8 (h)	$x00$; $\overline{x}00$; $0x0$; $0\overline{x}0$;
	8 (i)	$x0\frac{1}{2}$; $\overline{x}0\frac{1}{2}$; $0x\frac{1}{2}$; $0\overline{x}\frac{1}{2}$;
	8 (j)	$x,\frac{1}{2}+x,\frac{1}{4}$; $\overline{x},\frac{1}{2}-x,\frac{1}{4}$; $\overline{x},\frac{1}{2}+x,3/4$; $x,\frac{1}{2}-x,3/4$;
C_{4v}^{10}	16 (d)	xyz; $\overline{xy}z$; $\overline{y}xz$; $y\overline{x}z$; $\overline{x},y,\frac{1}{2}+z$; $x,\overline{y},\frac{1}{2}+z$;
		$y,x,\frac{1}{2}+z$; $\overline{y},\overline{x},\frac{1}{2}+z$;
	8 (c)	$x,\frac{1}{2}+x,z$; $x,\frac{1}{2}-x,z$; $\frac{1}{2}+x,\overline{x},z$; $\frac{1}{2}-x,x,z$;
C_{4v}^9	16 (e)	xyz; $\overline{xy}z$; $\overline{x}yz$; $x\overline{y}z$; yxz; $\overline{y}\overline{x}z$; $y\overline{x}z$; $\overline{y}xz$;
	8 (c)	xxz; $\overline{x}\overline{x}z$; $\overline{x}xz$; $x\overline{x}z$;
	8 (d)	$x0z$; $\overline{x}0z$; $0xz$; $0\overline{x}z$;
D_{2d}^{11}	16 (j)	xyz; $\overline{xy}z$; $\overline{x}y\overline{z}$; $x\overline{y}z$; $\overline{y}x\overline{z}$; $yx\overline{z}$; yxz; $\overline{y}\overline{x}z$;
	8 (f)	$x00$; $\overline{x}00$; $0x0$; $0\overline{x}0$;
	8 (g)	$x0\frac{1}{2}$; $\overline{x}0\frac{1}{2}$; $0x\frac{1}{2}$; $0\overline{x}\frac{1}{2}$;
	8 (i)	xxz; $\overline{x}\overline{x}z$; $\overline{x}\overline{x}\overline{z}$; $x\overline{x}\overline{z}$;
D_{2d}^{10}	16 (i)	xyz; $\overline{xy}z$; $\overline{y}x\overline{z}$; $y\overline{x}\overline{z}$; $\overline{x},y,\frac{1}{2}+z$; $x,\overline{y},\frac{1}{2}+z$;
		$y,x,\frac{1}{2}-z$; $\overline{y},\overline{x},\frac{1}{2}-z$;
	8 (e)	$xx\frac{1}{4}$; $\overline{x}\overline{x}\frac{1}{4}$; $x,\overline{x},3/4$; $\overline{x},x,3/4$;
	8 (h)	$x,\frac{1}{2}+x,0$; $\overline{x},\frac{1}{2}-x,0$; $x,\frac{1}{2}-x,\frac{1}{2}$; $\overline{x},\frac{1}{2}+x,\frac{1}{2}$;
D_{2d}^9	16 (j)	xyz; $\overline{xy}z$; $\overline{x}yz$; $x\overline{y}z$; $\overline{y}x\overline{z}$; $y\overline{x}\overline{z}$; $yx\overline{z}$; $\overline{y}\overline{x}\overline{z}$;
	8 (g)	$xx0$; $\overline{x}\overline{x}0$; $x\overline{x}0$; $\overline{x}x0$;
	8 (h)	$x,\frac{1}{2}+x,\frac{1}{4}$; $\overline{x},\frac{1}{2}-x,\frac{1}{4}$; $x,\frac{1}{2}-x,\frac{1}{4}$; $\overline{x},\frac{1}{2}+x,\frac{1}{4}$;
	8 (i)	$x0z$; $\overline{x}0z$; $0x\overline{z}$; $0\overline{x}\overline{z}$;

The determinat ı of the x and y parameters

All the sixteen-fold positions which are listed in table 2 belong
to the same (x,y) plane group, C4$\ell\ell$, and consequently, have the same
structure factor. Therefore, a plot of the structure factor, F, as a
function of x and y was made for one-sixteenth of the unit cell using
Lipson and Beevers strips (9). (This evaluation is similar to the one
suggested by Bragg and Lipson (10)). The plots were made for the strong
reflections (550),(11,5,0), (660), (10,6,0) and (510) and for the absent
reflections (12,2,0), (12,0,0), (880) and (770).[1]

The maximum F values on the plot were rated as 100. It was assumed
that parameter values of x and y which led to $/F/{<}20$ for the sixteen-
fold positions could not possibly account for the strong reflections
irregardless of the contribution of the atoms in the eight-fold posi-
tion. Similarly, values of x and y which gave $/F/{>}80$ for the sixteen-
fold position could not become absent reflections irregardless of the
contribution of the atoms in the eight-fold position. This method of
elimination led to the following possible x and y parameter values:
(Where x=y, the parameters correspond to an eight-fold position.)

	x	y
A	0.183	0.017
B	0.183	0.167
C	0.083	0.083
D	0.100	0.100
E	0.067	0.033
G	0.217	0.100

Parameters A and B did not lead to a suitable arrangement; C and D
corresponded to eight-fold positions. The arrangement E was eliminated
because it placed the uranium atoms too close together. Using para-
meter G a reasonable arrangement of uranium atoms was obtained as well
as a rough agreement with the intensity data. When the uranium atoms
in the sixteen-fold position were given the G parameter values, only
one of the eight-fold positions was favored by intensity calculations.

---

[1]The reflections (12,2,0) and (12,0,0) were later observed as
weak on a much more intense diagram taken with the crystal rotating
about (010).

Reasonable values for the x parameter for the uranium atoms in the eight-fold position seemed to be either 0.100 or 0.400 (corresponding to D). These parameters gave very reasonable agreement with the intensity data.

In order to refine the values of the parameters, a projection of the electron density upon (001) was made by evaluating the double Fourier series,

$$\rho(x,y)=\sum_h \sum_\kappa F_{(\underline{hk}0)} e^{-2\pi i(\underline{h}x+\underline{k}y)}$$

The signs of the $F_{(\underline{hk}0)}$ were determined from the F's calculated on the basis of the approximate parameters found above. The parameters which are listed below were determined from the positions of the peaks in the electron density map illustrated in figure 1. Small peaks due to the M atoms were found at the origin and center of the projection. Calculation of the structure factor using the new parameters did not require the change in sign of any term used in the Fourier series. Thus, the parameters for the positions listed below are the best that can be obtained by this treatment of the (hk0) intensity data.

(Add $00, \frac{11}{22}$ to all positions)

4 M   at   00;   00;

16 U   at   xy; $\overline{xy}$; $\overline{x}y$; $x\overline{y}$; yx; $\overline{yx}$; $\overline{y}x$; $y\overline{x}$;
with x = 0.2141,   y = 0.1021

8 U   at $x,\frac{1}{2}+x$; $\overline{x},\frac{1}{2}-x$; $\frac{1}{2}+x,\overline{x}$; $\frac{1}{2}-x,x$;
with x = 0.4068

The observed ratio of the average heights of the peaks of electron density due to the uranium atoms to those due to the two M atoms is 92/55 after correction for the valleys in the Fourier projection. Since the plot was made using intensity data from U_6Mn, the ratio should be approximately 92/50. The projection was made several times from several sets of intensity data corrected in different ways for the absorption factor. The positions of the peaks were the same in each case within several ten-thousandths of a unit cell dimension. Although the absorption factor did not seem important to the determination of the parameter values by this method, the agreement between calculated and observed intensities was very dependent upon the absorption factor.

The amplitude data were treated only once by the least squares method (11). The parameters obtained in this case were x = 0.2134,
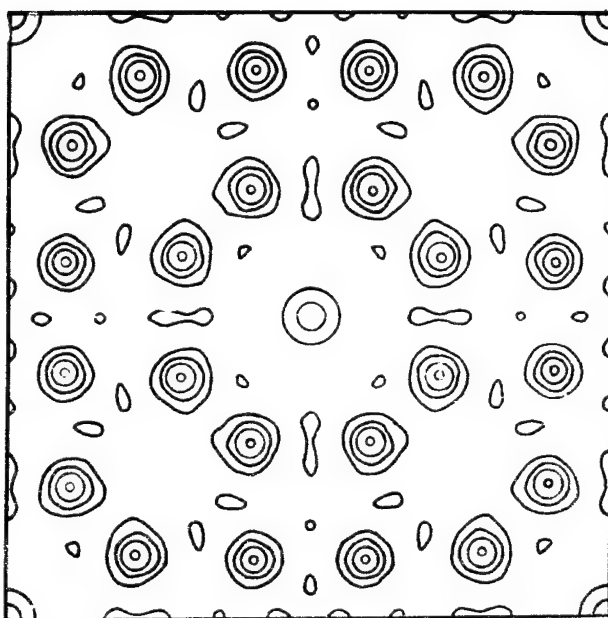
Fig. 1--Electron density of U$_6$M projected
on (001).

$y = 0.1065$ for the sixteen-fold position and $x = 0.4053$ for the eight-fold position. A third more-or-less trial and error refinement made preceding the Fourier projection gave the values 0.213, 0.103, and 0.405.

Actually, it is difficult to say which set of parameters gives the best agreement with the intensity data. The first and last set of parameters permit more reasonable uranium-uranium distances than the second set. Only one least squares determination was performed which may explain the high value of the $\underline{y}$ parameter obtained by that method.

The parameter values determined from the electron density plot were used to calculate the intensities of the ($\underline{hk}$0) reflections for comparison with the observed values as shown in table 3.

The determination of the z parameters

The determination of the x and $\underline{y}$ coordinates of the atoms eliminated space groups D_{4h}^{17}, D_{2d}^{11}, D_{2d}^{9}, and C_{4v}^{9} since the sixteen-fold positions in these space groups place atoms impossibly close together in the same plane. Most of the eight-fold positions were eliminated for similar reasons. The decision between the remaining space groups depended upon the arrangement in the $\underline{z}$ direction.

There are only four different arrangements in the z direction, all of which are very close to the arrangement in space group D_{4h}^{18}. In this space group two uranium atoms in the sixteen-fold position are placed only 2.69 A apart. The arrangement in C_{4v}^{10} does not permit an enlargement of this distance, and there seems to be no other reason for considering this set of positions further. The arrangements in both D_{2d}^{10} and D_{4}^{9} permit this distance to be enlarged, since the z parameter allows variation from the parameterless positions in D_{4h}^{18}. There is an optimum value of this parameter which places the two uranium atoms a maximum distance apart (2.73 A. in each case) with $z = 0.042$ for D_{2d}^{10} and $z = 0.208$ for D_{4}^{9}. Increasing or decreasing the value of this $\underline{z}$ parameter places two uranium atoms closer together.

It should be possible to distinguish among these four possibilities and to determine the z parameter on the basis of the (00ℓ), (hkℓ) or (0kℓ) data. Unfortunately, here, as in the case of the (hk0) data, the absorption factor was very important, and it was even more difficult to

Table 3

Intensity Comparisons for U_6Mn: (hk0) Data

Indices	Calculated	Observed
110	28.3	*
200	3.3	15
220	29	32
310	31.7	32
400	89.7	60
330	102	100
420	120	120
510	336	200
440	49	50
530	22.3	20
600	186	75
620	16.4	15
710	4.7 ⎤	900
550	1290 ⎦	
640	66.6	100
730	19	50
800	1.6	--
820	12.6	15
660	214	185
750	25.7	40
840	79.2	70
910	23.4	25
930	61.4	65
770	4	5
10,0,0	149 ⎤	190
860	8 ⎦	
10,2,0	7.4	10
950	44.8	35

*Not observed on this film because of the beam catcher. It has been observed on other films in about the right magnitude.

Table 3

(Continued)

Indices	Calculated	Observed
10,4,0	32.1	30
11,1,0	150	160
880	8.1	——
11,3,0	1.3]	
970	86.3]	50
10,6,0	417	400
12,0,0	1.4	——
11,5,0	1160	850
12,2,0	9.9	——
12,4,0	60.6	60
990	317	170

calculate. It was, however, carefully calculated for the (00ℓ) data.
From the comparison of the estimated and calculated intensities given in
table 4, it is evident that the z parameter differs less than 0.02 from
the ideal values of zero and one-fourth for D_{2d}^{10} and D_4^9 respectively.
The temperature factor was omitted in these calculations; if it is
appreciable, it will require the parameter to differ even less from the
ideal values.

With this small variation it becomes difficult to choose between
the arrangements in D_4^9 and D_{2d}^{10}. The arrangement in D_{2d}^{10} seems more prob-
able because it does not permit the reflections of the type $(0k\ell)$ with
k and ℓ odd to occur at all. These reflections are not observed. In
fact, since the parameter seems near zero, it is quite possible that
the arrangement in D_{4h}^{18} is correct. Intensities have been calculated
for the (hkl) reflections on the basis of the D_{4h}^{18} arrangement using the
absorption correction cited previously and are given in table 5. The
agreement is only fair; the discrepancies are undoubtedly due to the
approximate absorption correction.

Table 4

Intensity Comparisons for U_6M: $(00\underline{\ell})$ Data

Indices	$\underline{z} = 0.00$	Calculated 0.02	0.04	Observed
002	606	680	1030	630
004	260	260	260	260
006	242	186	59	195

Table 5

Intensity Comparisons for U_6M: $(\underline{hk}l)$ Data

Indices	Calculated	Observed
101		
211	0.6	0
301	0	0
321	858	900
611	32	40
501	0	0
431	34	60
521	2.7	20
611	45	50
541	0.2	0
631	0.3	0
701	0	0
721	85	100

Table 5

(Continued)

Indices	Calculated	Observed
651	2.8	0
811	1.5⎤	
741	3.6⎦	15
831	627	500
901	0	0
921	23 ⎤	
961	52 ⎦	75
851	6.8	20
941	17.7	0
10,1,1	0.5	0
10,3,1	19	35
871	454	250
961	30	25
11,0,1	0	0
11,2,1	11.3⎤	
10,5,1	5.7⎦	15
11,4,1	132	100

Discussion of the Structure

Interatomic distances

The interatomic distances in this structure have been calculated
for an average value of the unit cell dimensions of the four iso-
structural compounds, $a = 10.34$ A., $c = 5.21$ A. These distances are
listed in table 6. One of the notable points in this table is the close
uranium-uranium distances which are observed. The distance between the

U_1 atoms of 2.69 A. is 0.07 A. less than the shortest distance observed in uranium metal (2.76 A.) (12). (From the limits of error set on the value of the $\underline{y}$ parameter in the uranium metal structure, this distance could be as low as 2.74 A.) Even the distance between the U_2 atoms of 2.73 A. is less than that observed in uranium metal.

Table 6

Interatomic Distances in the U_6M Compounds
(in Angstroms)

| U_1 Ligands | | | U_2 Ligands | | | M Ligands | | |
Ligands		Distance	Ligands		Distance	Ligands		Distance
1	U_1	2.69	1	U_2	2.73	2	M	2.61
2	M	2.78	2	U_1	2.84	8	U_1	2.78
1	U_2	2.84	4	U_2	3.24			
2	U_1	3.08	4	U_1	3.28			
2	U_2	3.28	2	U_1	3.39			
2	U_1	3.35						
1	U_2	3.39						
2	U_1	3.47						

It is interesting to see what results are obtained when Pauling's metallic radii and his relationship between bond order and radii are applied to this structure (13). Using the radius of 1.42 for uranium and an average value of 1.16 for the radius of the transition metal atom, the bond orders were calculated according to the formula

$$R(1) - R(n) = 0.30 \log n ,$$

where $R(1)$ is the single bond radius of Pauling, $R(n)$ is the radius of an atom participating in an $\underline{n}$th order bond. The short distance of 2.69 A. corresponds to a 1.8 bond.

The valence of each kind of atom can be found by summing up all the bond orders of the bonds which the atom forms with its neighbors. The valence of the U_1 atoms was found to be 5.46; the valence of the U_2 atoms was found to be 5.36. These valences are in quite reasonable agreement with Pauling's value of 5.78 for uranium. The valence of the

transition metal atom, 4.50, is not in agreement with the expected value of 5.78. Its value can be increased in the D_{2d}^{10} and D_4^9 arrangements, however.

Application of the zone theory of metals

Hume-Rothery (14) found that certain metal alloy phases achieved stability when they had a fixed electron to atom ratio. Jones (15,16) tried to explain this observation on the basis of the modern zone theory of metals. He found that for alloy phases which satisfied Hume-Rothery's rule, the edge of the filled region of energy levels was close to a prominent zone boundary. Thus, Hume-Rothery's rule is equivalent to stating that a stable alloy phase occurs if there is a nearly filled system of zones.

Jones showed qualitatively that the stability of the phase increased up to the point where the energy contours in wave-number space touched the zone boundary. In filling up the remaining levels the average energy of the additional energy is larger than the mean energy of all the electrons. Thus, the stability of the phase decreases as the rest of the energy levels in the zone are filled up. The stability of the nearly filled zone is more apparent if there is a large discontinuity in the energy of the levels at the zone boundary. Jones showed that a large value of the structure amplitude (as used in X-ray diffraction) is essential for a large energy discontinuity. Thus, the important zone is that zone bounded by planes corresponding to the strong X-ray reflections.

The vector equation of the planes forming the zone boundaries is
$$\vec{K} \cdot \vec{K} = \vec{K}^2/4,$$
where $\vec{K}$ is the running vector in the reciprocal lattice, and $\vec{K}$ is the reciprocal lattice vector, $h\vec{a}* + k\vec{b}* + l\vec{c}*$, to the point (hkl) in the reciprocal lattice corresponding to the planes with strong X-ray reflections. Each element of "K" space, the unit volume in reciprocal lattice space, contains one electron pair. Thus, the number of electron pairs which can be placed in energy levels before a particular zone boundary is reached is equal to the volume of the space encompassed by the zone boundary divided by the unit volume of "K" space.

There is, apparently, some difference of opinion concerning the correct valences and the important volume to be considered in applying the zone theory. Jones used the valences of Hume-Rothery and considered

the volume of the sphere inscribed in the zone as being of primary importance. Pauling (17) used his valences and considered the filling of the whole zone to be important. Frequently, the difference in volume between the inscribed sphere and the zone are not large. Pauling's valence for the transition metals, however, is 5.78, while on Hume-Rothery's scheme it is zero.

The important planes in the U_6M structure are the (002), (004), (550), (552), (321), (323), (600), (660), (10,0,0), (11,5,0), (831), and (10,6,0) planes. If one uses Pauling's valences, there are $(24+4) \times 5.78$ or 161.8 electrons in the unit cell. Since there are 2 electrons per unit of "K" space, in this case $a*^2c*$, the unit volume of the reciprocal lattice space, the volume of a filled zone should be 80.9 $a*^2c*$. Using the valence of six for uranium and zero for the transition metal atom, there would be 144 electrons in the unit cell. From the observed values of the valence, the number of bonding electrons is 148.7. The radius of the sphere in reciprocal lattice space which would contain the proper number of electrons is 3.37 $a*$ for the case using Pauling's values of the valences. The radii would be slightly smaller for the other cases. This radius corresponds roughly to the normal distance from the origin to the zone boundaries due to a (550) plane, for which the distance is 3.535 $a*$, or to the (323) plane, for which the distance is 3.48 $a*$, or to the (600) plane for which the distance is 3 $a*$.

The volumes of the possible bounding zones have been calculated and are listed in table 7. Only one of the zones has the correct value on any basis. The zone bounded by the planes due to (600) and (002) will hold 144 electrons. This is the number obtained by using Hume-Rothery's valences. However, this zone is truncated by many other zones.

Table 7

Volumes of the Important Zones in U_6M Compounds

Zone Boundary Planes	Volume
(321)	61.6 $a*^2c$
(600)　(002)	72.
(550)　(002)	100.
(550)　(323)	127.

Most of the zones have a much larger volume than those shown in table 7.

Probably the zone theory does not have any real significance for this structure. Even if it does, it does not seem immediately evident that this theory should predict the absence of a similar structure in the uranium-chromium system or even in the uranium-copper system.

Conclusions

1. The crystal structure of the isostructural compounds, U_6Mn, U_6Fe, U_6Co, and U_6Ni, has been determined.

2. The structure has been considered from the viewpoint of the theories of metals. Pauling's suggestions concerning the valence and metallic radii seem to be consistent with this structure. The applicability of the zone theory of metals to this compound is questionable.

Summary

The unit cell dimensions and structure of the isostructural compounds, U_6Mn, U_6Fe, U_6Co, and U_6Ni, have been determined. The dimensions of the body-centered tetragonal unit cell for U_6Mn are $a = 10.29$ A., $c = 5.24$ A.; for U_6Fe, $a = 10.31$ A., $c = 5.24$ A.; for U_6Co, $a = 10.36$ A., $c = 5.21$ A.; for U_6Ni, $a = 10.37$ A., $c = 5.21$ A. The atomic positions may be described on the basis of positions of space group D_{4h}^{18} with the atoms in the following positions:

(Add $000, \frac{111}{222}$ to all positions)

4 M at $00\frac{1}{4}$; $003/4$

16 U at $xy0$; $\overline{xy}0$; $\overline{y}xo$; $y\overline{x}0$; $\overline{xy}\frac{1}{2}$; $x\overline{y}\frac{1}{2}$; $yx\frac{1}{2}$; $\overline{yx}\frac{1}{2}$;
with $x = 0.2141$, $y = 0.1021$

8 U at $x, \frac{1}{2}+x, \overline{0}$; $\overline{x}, \frac{1}{2}-x, \overline{0}$; $\frac{1}{2}+x, \overline{x}, 0$; $\frac{1}{2}-x, x, 0$;
with $x = 0.4068$.

A possible variation from these positions in space groups D_4^9 and D_{2d}^{10} has not been eliminated.

The structure is discussed from the viewpoint of the theory of metals.

THE STRUCTURE OF THE Th_7M_3 COMPOUNDS

Introduction

The binary systems of thorium with the first transition group metals have not been investigated as extensively as their uranium analogs. No X-ray data has been reported, and only fragmentary thermal and microscopic investigations have been made. Thus, none of the compositions of the intermetallic phases were known at the start of these structural investigations.

The Determination of the Composition of Th_7M_3

Preparation and occurrence

The alloys were prepared in the same fashion as the uranium alloys in the preceding section. Similarly, alloys with less than 70 atomic per cent thorium provided single crystals of the compound. The single crystals existed in the form of six-sided needles protruding into cavities in the alloy. The needles were brittle and were easily separated from the rest of the alloy.

The compounds were found to occur in the systems of thorium with iron, cobalt, and nickel. A suitable alloy which might contain the manganese analog of these compounds has not yet been prepared. Powder diagrams of the alloys were almost identical for all three compounds. In addition, the single crystal rotation diagrams of each of the compounds appeared similar.

The composition of Th_7M_3

The composition of the thorium-iron compound was determined by a combination of microscopic and X-ray diffraction methods. It was assumed that the volume occupied by the thorium and iron atoms in the intermetallic compound was the same as that in the primary phases (6). The atomic volume of thorium is 32.9 A^3; the atomic volume of iron is 11.8 A^3 The volume of the unit cell of the compound (see below), 518 A^3, is only slightly smaller than the volume of sixteen thorium atoms (525.8 A^3).

Since the volume of one thorium atom is about three times that of an iron atom, the removal of one thorium atom and the substitution of three iron atoms will leave the total volume of the unit cell almost unchanged. The series of compositions which result together with the expected volume of the unit cell are given in table 8.

Table 8

Possible Compositions for the Thorium-Iron Compound

Composition	Volume of unit cell in A^3	Atomic % Fe
Th_{16}	525.8	0
$Th_{15}Fe_3$	528.3	16.7
$Th_{15}Fe_2$	516.5	11.8
$Th_{14}Fe_6$	530.9	30.0
$Th_{14}Fe_5$	519.0	26.3
$Th_{14}Fe_4$	506.2	22.2
$Th_{13}Fe_9$	533.3	40.9
$Th_{13}Fe_8$	521.5	38.1
$Th_{13}Fe_7$	509.7	35.0
$Th_{12}Fe_{12}$	535.7	50.0
$Th_{12}Fe_{11}$	523.7	47.8
$Th_{12}Fe_{10}$	512.2	45.4

Microscopic evidence indicated that the composition of the phase was in the neighborhood of twenty-eight atomic per cent iron. Only two compositions of the atoms in the unit cell are compatible with the microscopic evidence, $Th_{14}Fe_6$ and $Th_{14}Fe_5$. The final choice between these two compositions depends on the structural investigation. From the investigation of the structure presented below it is evident that six is the proper number of iron atoms in the unit cell.

X-ray Diffraction Data

Experimental methods

Equipment and source of X-rays. The equipment and source of X-rays were the same as in the previous section.

Intensity determination and correction. The (hk0),(hkl), and (hk2) reflections were obtained from rotation diagrams taken with the crystal rotating about the c axis. Numerical values were assigned to the (hk0) maxima by visual comparison with a series of spots of known intensities. The intensities of the (hkl) and (hk2) reflections were determined by the method described in part five of this thesis. Intensity data from rotation about axes normal to the needle axis were not obtained because of the unreliability of the absorption corrections which would be necessary.

The $F^2/\bar{f}^2$ coefficients for the Patterson series were determined from the observed intensities by the following relationship,

$$F^2/\bar{f}^2 \propto I/LPMA\bar{f}^{\,2},$$

where I is the observed intensity; LP, the Lorentz and polarization factors; M, the multiplicity factor; A, the absorption factor; $\bar{f}$, the mean atom form factor as defined by Patterson (18); and F, the structure factor.

The experimental structure factors which form the coefficients of the Fourier series were determined by the formula

$$|F| \propto \sqrt{I/LPMA}\,.$$

The calculated (hk0) intensities shown in comparison with the observed values in table 11 were calculated according to the relationship

$$I \propto FF*LPMA,$$

where F* is the complex conjugate of F. The same relationship was used for calculating the (hkl) and (hk2) intensity data except that the Lorentz factor included the Ott velocity factor. All absorption corrections were made on the assumption that the needle was a cylindrical rod. No temperature factor corrections were made.

Unit cell dimensions

The single crystals of the thorium-iron compound were examined by Wilson by the rotating single crystal method. From these X-ray diagrams

the unit cell dimensions were found to be $\underline{a}$ = 9.85 A., $\underline{c}$ = 6.15 A. for a hexagonal unit cell. The single crystals of the thorium-cobalt and thorium-nickel compounds produced almost identical diffraction patterns.

The unit cell dimensions determined by the single crystal method enabled the powder diagrams of these phases to be interpreted. The unit cell dimensions of the compounds in the thorium-iron, thorium-cobalt, and thorium-nickel systems have been determined from powder diagrams by A. I. Snow. The unit cell dimensions are listed in table 9.

Table 9

Unit Cell Dimensions of the Th_7M_3 Compounds[a]
(in Angstroms)

Compound	$\underline{a}$	$\underline{c}$
Th_7Fe_3	9.85	6.15
Th_7Co_3	9.83	6.17
Th_7Ni_3	9.86	6.23

[a]The dimensions are expressed in true Angstrom units (8).

Laue symmetry

Oscillation diagrams taken with the crystal rotating about the $\underline{c}$ axis showed that the crystal possessed a mirror plane perpendicular to the six-fold axis. De Jong-Bouman diagrams, prepared by A. I. Snow, showed that the crystal possessed six mirror planes parallel to the six-fold axis. The Laue symmetry is, then, D_{6h}.

Structural Determination

Space group determination

Only space groups which produce the diffraction symmetry of D_{6h} and which provide positions for fourteen thorium atoms in the unit

cell need to be considered. The thorium atoms may be represented by a twelve-fold set plus a two-fold set of equivalent positions, or two six-fold plus one two-fold set of positions. The occurrence of a combination of three- or four-fold sets is less likely.

The only systematically absent reflections are the $(hk\ell)$ reflections with $\underline{h} - \underline{k} = 3n$, $\underline{\ell} = 2n + 1$. Since the iron atoms do not have a large scattering power relative to the thorium atoms, this extinction applies primarily to the thorium atom positions.

The unit cell dimensions are such that it is impossible to place two thorium atoms above one another along the $\underline{c}$ axis. The sum of the diameters of two thorium atoms is 7.17 A.; the observed $\underline{c}$ dimension is approximately 6.1 to 6.2 A. In addition, it would be impossible to place twelve thorium atoms all in the same plane in the unit cell. Even if one would assume that three thorium atoms could lie along each edge (three thorium diameters = 10.76 A., the unit cell dimension is 9.9A.), there would only be nine thorium atoms in the one plane of the unit cell.

As a result of the restrictions concerning the number of atoms, the general extinctions, and the spatial requirements of the thorium atoms, only the twelve- and six-fold positions listed in table 10 are available for the thorium atoms in the unit cell.

Determination of the x and y parameters

The position of two thorium atoms in the (x,y) plane is clearly determined to be at $(1/3, 2/3)$ and $(2/3, 1/3)$. In order to select the proper set of positions for the remaining thorium atoms and to determine the approximate values of the parameters, a Patterson $F^2/\underline{f}^2$ vector map (18) was prepared by evaluating the expression

$$p(x,y) = \sum_{-\infty}^{\infty} \sum_{-\infty}^{\infty} F^2/\bar{f}^2{}_{\underline{hko}} \ e^{2\pi i(\underline{hx} + \underline{ky})}$$

A contour plot of this projection is shown in figure 2. The plane group of the projection is C6$\ell\ell$.

Most of the peaks on the plot are representable by the general coordinates $(x,2x)$, $(2x,x)$, $(x,\bar{x})$. Only a few minor peaks have coordinates $(x,0)$, $(0,x)$, (x,x), or the general coordinate (x,y). In general, the peaks due to vector distances between atoms in the twelve-fold general position of the C6$\ell\ell$ plane group have the coordinates listed below plus

those arising from the symmetry of the plane group.

$$
\begin{array}{ll}
x + y, & x + y \\
2x - y, & 2x - y \\
x - 2y, & x - 2y \\
x, & \overline{x} \\
y, & \overline{y} \\
x - y, & y - x \\
x, & y \\
x + y, & 2x - y \\
2x, & 2y
\end{array}
$$

Table 10

Possible Atomic Positions for Th_7M_3

Space group		Positions
D_{6h}^4	12 (j)	$xy\frac{1}{4}$; $\overline{y},x - y,\frac{1}{4}$; $y - x,\overline{x},\frac{1}{4}$; $\overline{x},\overline{y},3/4$; $y,y - x, 3/4$;
		$x - y,x,3/4$; $y,x,3/4$; $\overline{x},y - x,3/4$; $x - y,\overline{y},3/4$;
		$\overline{y},\overline{x},\frac{1}{4}$; $x,x - y,\frac{1}{4}$; $y - x,y,\frac{1}{4}$;
	6 (h)	$x,2x,\frac{1}{4}$; $2\overline{x},\overline{x},\frac{1}{4}$ $x,\overline{x},\frac{1}{4}$; $\overline{x},2\overline{x},3/4$; $2x,x,3/4$; $\overline{x},x,3/4$;
	2 (c)	$1/3,2/3,\frac{1}{4}$; $2/3,1/3,3/4$;
	2 (d)	$1/3,2/3,3/4$; $2/3,1/3,1/4$;
D_{6h}^1	6 (m)	$x,2x,\frac{1}{2}$; $2\overline{x},\overline{x},\frac{1}{2}$; $x,\overline{x},\frac{1}{2}$; $\overline{x},2\overline{x},\frac{1}{2}$; $2x,x,\frac{1}{2}$; $\overline{x},x,\frac{1}{2}$;
	6 (l)	$x,2x,0$; $2\overline{x},\overline{x},0$; $x,\overline{x},0$; $\overline{x},2\overline{x},0$; $2x,x,0$; $\overline{x},x,0$;
	6 (k)	$x,0,\frac{1}{2}$; $0,x,\frac{1}{2}$; $\overline{x},\overline{x},\frac{1}{2}$; $\overline{x},0,\frac{1}{2}$; $0,\overline{x},\frac{1}{2}$; $x,x,\frac{1}{2}$;
	6 (j)	$x,0,0$; $0,x,0$; $\overline{x},\overline{x},0$; $\overline{x},0,0$; $0,\overline{x},0$; $x,x,0$;
	2 (c)	$1/3,2/3,0$; $2/3,1/3,0$;
	2 (d)	$1/3,2/3,1/2$; $2/3,1/3,1/2$;
D_6^1	12 (n)	x,y,z; $\overline{y},x - y,z$; $y - x,\overline{x},z$; $\overline{x},\overline{y},z$; $y,y - x,z$;
		$x - y,x,z$; $y,x,\overline{z}$; $\overline{x},y - x,\overline{z}$; $x - y,\overline{y},z$; $\overline{y},\overline{x},\overline{z}$;
		$x,x - y,\overline{z}$; $y - x,y,\overline{z}$;

The six-fold positions (m), (l), (k), and (j) and the
two-fold positions (d) and (d) are the same as in D_{6h}^1.

| C_{6v}^4 | 12 (d) | x,y,z; $\overline{y},x - y,z$; $y - x,\overline{x},z$; $\overline{x},\overline{y},\frac{1}{2}+z$; $y,y - x,\frac{1}{2} +x$; |

Table 10

(Continued)

Space group	Positions

$x - y, x, \frac{1}{2} + z; \quad y, x, \frac{1}{2} + z; \quad \overline{x}, y - x, \frac{1}{2} + z; \quad x - y, \overline{y}, \frac{1}{2} + z;$
$\overline{y}, \overline{x}, z; \quad x, x - y, z; \quad y - x, y, z;$

6 (c) $x, 2x, z; \quad 2\overline{x}, \overline{x}, z; \quad x, \overline{x}, z; \quad \overline{x}, 2\overline{x}, \frac{1}{2} + z; \quad 2x, x, \frac{1}{2} + z;$
$\overline{x}, x, \frac{1}{2} + z;$

2 (b) $1/3, 2/3, z; \quad 2/3, 1/3, 1/2 + z;$

C_{6v}^1 6 (e) $x, 2x, z; \quad 2\overline{x}, \overline{x}, z; \quad x, \overline{x}, z; \quad \overline{x}, 2\overline{x}, z; \quad 2x, x, z; \quad \overline{x}, x, z;$

         6 (d) $x, 0, z; \quad 0, x, z; \quad \overline{x}, \overline{x}, z; \quad \overline{x}, 0, z; \quad 0, \overline{x}, z; \quad x, x, z;$

         2 (b) $1/3, 2/3, z; \quad 2/3, 1/3, z;$

D_{3h}^4 6 (h) $x, y, \frac{1}{4}; \quad \overline{y}, x - y, \frac{1}{4}; \quad y - x, \overline{x}, \frac{1}{4}; \quad y, x, 3/4; \quad \overline{x}, y - x, 3/4;$
$x - y, \overline{y}, 3/4;$
The two-fold sets are the same as in D_{6h}^4

D_{3h}^3 6 (k) $x, y, \frac{1}{2}; \quad \overline{y}, x - y, \frac{1}{2}; \quad y - x, \overline{x}, \frac{1}{2}; \quad y, x, \frac{1}{2}; \quad \overline{x}, y - x, \frac{1}{2};$
$x - y, \overline{y}, \frac{1}{2};$

         6 (j) $x, y, 0; \quad \overline{y}, x - y, 0; \quad y - x, \overline{x}, 0; \quad y, x, 0; \quad \overline{x}, y - x, 0;$
$x - y, \overline{y}, 0;$

         2 (c) $1/3, 2/3, 0; \quad 2/3, 1/3, 0;$

         2 (d) $2/3, 1/3, 1/2; \quad 1/3, 2/3, 1/2;$

D_{3h}^1 6 (m) $x, y, \frac{1}{2}; \quad \overline{y}, x - y, \frac{1}{2}; \quad y - x, \overline{x}, \frac{1}{2}; \quad \overline{y}, \overline{x}, \frac{1}{2}; \quad x, x, y, \frac{1}{2};$
$y - x, y, \frac{1}{2};$

         6 (l) $x, y, 0; \quad \overline{y}, x - y, 0; \quad y - x, \overline{x}, 0; \quad \overline{y}, \overline{x}, 0; \quad x, x, y, 0;$
$y - x, y, 0;$

         2 (h) $1/3, 2/3, z; \quad 2/3, 1/3, \overline{z};$

         2 (i) $2/3, 1/3, z; \quad 1/3, 2/3, \overline{z};$

All of the possible x and y parameter values may be found from the $(x, \overline{x})$ set of peaks on the Patterson vector map. The possible values of x or y are 0.07, 0.13, 0.20, 0.26, 0.33, 0.40, 0.47, 0.53, 0.60, 0.67, 0.74, 0.80, 0.87, and 0.93. For any pair of x and y values chosen from the group, peaks with the general coordinates listed above plus those due to the plane group symmetry must occur if the choice is a proper one.
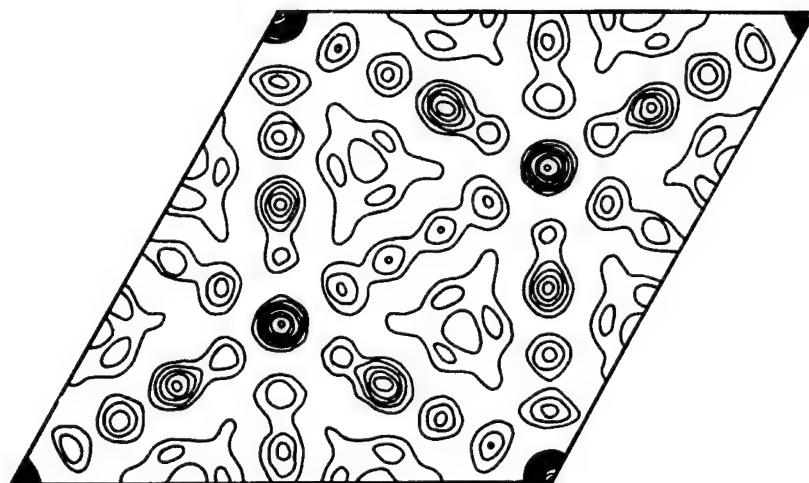
Fig. 2--Patterson projection of Th_7M_3 on (001).

38

It was found that the only combinations of $\underline{x}$ and $\underline{y}$ which would produce the other peaks were those which caused the general twelve-fold set of positions to pass over to a six-fold set of the type.

$$x, 2x; \quad 2x, x; \quad x, \overline{x}; \quad \overline{x}, 2\overline{x}; \quad 2\overline{x}, \overline{x}; \quad \overline{x}, x.$$

By trying the different possible parameter values in the six-fold positions, keeping in mind a satisfactory arrangement of the atoms with respect to interatomic distances, it was found that the following positions satisfied intensity and spatial requirements.

6 Th at $x, 2x; \quad 2x, x; \quad x, \overline{x}; \quad \overline{x}, 2\overline{x}; \quad 2\overline{x}, \overline{x}; \quad \overline{x}, x;$
with $\underline{x} = 0.122$ or 0.878.
6 Th at the same set of positions but with $\underline{x} = 0.456$
or 0.544.
2 Th at $1/3 \; 2/3; \; 2/3 \; 1/3$.

The iron atoms were placed in holes in the structure with the positions,
6 Fe at $x, 2x; \quad 2x, x; \quad x, \overline{x}; \quad \overline{x}, 2\overline{x}; \quad 2\overline{x}, \overline{x}; \quad \overline{x}, x;$
with $\underline{x} = 0.167$ or 0.833.

These positions are in accord with the Patterson diagram, and peaks are present on the diagram at the actual positions of the thorium atoms above. This is to be expected as the result of vectors from the thorium atoms at $(1/3, 2/3)$ and $(2/3, 1/3)$.

The structure factors for the approximate positions found above were calculated for (hk0) reflections. The signs of the structure factors were used with the observed values of the structure factor in the Fourier series representing the projection of the electron density along the $\underline{c}$ axis on to the (x, y) plane. As a result of these summations, the better values of the parameters as determined from the positions of maximum electron density in the plot were found to be $\underline{x} = 0.126$, $\underline{x}' = 0.539$ for the thorium atoms and $\underline{x} = 0.800$ for the iron atoms.

Determination of the z parameters

As a result of consideration of the spatial requirements of the thorium atoms, there appears to be only two methods of arranging the atoms in the $\underline{z}$ direction.

Arrangement I

2 Th at $1/3, 2/3, 1/4; \quad 2/3, 1/3, 3/4;$
6 Th at $x, 2x, \frac{1}{4}; \quad 2x, x, 3/4; \quad 2\overline{x}, \overline{x}, \frac{1}{4}; \quad \overline{x}, 2\overline{x}, 3/4; \quad x, \overline{x}, \frac{1}{4};$
$\overline{x}, x, 3/4; \quad$ with $\underline{x} = 0.126$

6 Th at same positions with $\underline{x} = 0.539$
6 Ni at same positions with $\overline{\underline{x}} = 0.800$.

Arrangement II

2 Th at $1/3,2/3,z$; $2/3,1/3,1/2+z$; with $\underline{z} \approx 0$
6 Th at $x,2x,z$; $2\overline{x},\overline{x},z$; $x,\overline{x},z$; $\overline{x},x,\frac{1}{2}+z$; $\overline{x},2\overline{x},\frac{1}{2}+z$;
      $2x,x,\frac{1}{2}+z$; with $\underline{x} = 0.126$ and $\underline{z} \approx 0.250$
6 Th at the same positions with $\underline{x} = 0.539$ and $\underline{z} \approx 0$
6 M at the same positions with $\overline{\underline{x}} = 0.800$ and $\overline{\underline{z}} \approx 0.250$.

The structure factor for the (hk2) reflections is the same except
for sign as that for (hk0) reflections for the arrangement I. Therefore,
if this arrangement existed, the intensities of the (hk2) reflections
should parallel those of the (hk0) reflections. The intensity data
definitely reject this arrangement, however, as the second layer line,
as well as the first layer line, in the single crystal rotation diagrams
is strikingly different from the zero layer line.

The intensities of the (hk1) and (hk2) reflections calculated on the
basis of arrangement II using the ideal $\underline{z}$ parameter values appear to
agree satisfactorily with the observed intensities. In order to determine
the existence of a deviation from these ideal parameter values, more ex-
tensive (hkℓ) and (00ℓ) data would be necessary. Since the crystal's
needle axis is parallel to the $\underline{c}$ axis, the absorption correction becomes
a serious factor in intensity calculations. The accuracy of determining
the $\underline{z}$ parameters would resolve into the accuracy of determining the ab-
sorption factor.

If, however, one does not provide for a variation from the ideal
values of the $\underline{z}$ parameter, as listed above, several atoms are placed very
close together in the structure. Therefore, $\underline{z}$ parameters have been varied
to place the atoms further apart. Also, the $\overline{\underline{x}}$ parameter for the thorium
atoms in one six-fold set of positions was changed because two thorium
atoms described by the same set of positions were very close together.
The iron atom parameters were adjusted in both the $\underline{x}$ and $\underline{z}$ directions to
produce reasonable interatomic distances between atoms. The optimum set
of parameters with regard to distance together with the positions are
listed below.

2 Th at $1/3,2/3,z$; $2/3,1/3,1/2+z$; with $\underline{z} = 0.06$
6 Th at $x,2x,z$; $2\overline{x},\overline{x},z$; $x,\overline{x},z$; $\overline{x},x,\frac{1}{2}+z$; $\overline{x},2\overline{x},\frac{1}{2}+z$;
      $2x,x,\frac{1}{2}+z$; with $\underline{x} = 0.126$ and $\underline{z} = 0.250$
6 Th at the same positions with $\underline{x} = 0.544$ and $\underline{z} = 0.03$
6 M at the same positions with $\overline{\underline{x}} = 0.815$ and $\overline{\underline{z}} = 0.31$.

A projection of these atomic positions upon the (x,y) plane is shown in figure 3. The calculated intensities of the $(\underline{hk}0)$, $(\underline{hk}1)$ and $(\underline{hk}2)$ re-flections agree with the observed values as well as may be expected in view of the absorption approximation. The intensity comparisons are shown in tables 11, 12, and 13.

Discussion of the Structure

Interatomic distances

Interatomic distance calculations already have played a part in determining the final structure. Nevertheless, it is still instructive to apply Pauling's rule relating bond number to bond distance. The bond numbers were calculated for all the bond distances connecting each type of thorium atom as shown in table 14. The valences of the atoms, which were found by summing up all the bond orders of the bonds to the atom concerned, are 4.03 for Th_I, 4.44 for Th_{II}, and 3.42 for Th_{III}. This is reasonable agreement with the expected value of 4. The valence of the transition metal atom, 4.23, again is low as in the uranium compounds. The accuracy of placement of this kind of atom is not nearly as great as for the thorium atoms, however.
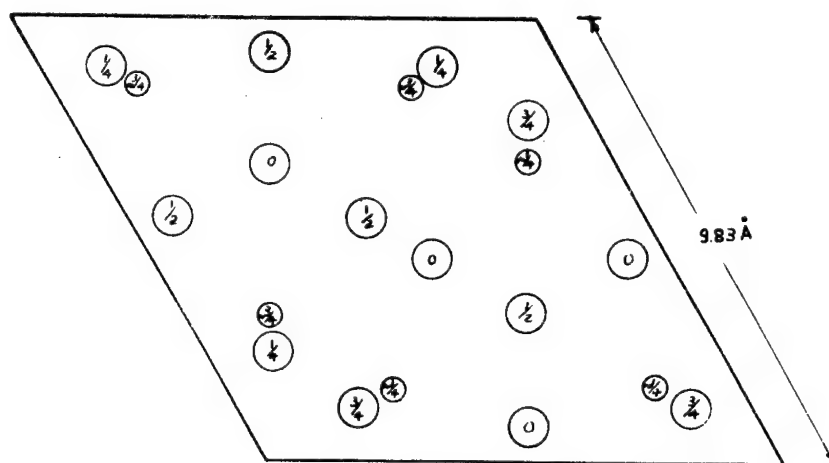
Fig. 3--The projection of the Th_7M_3 structure on (001). (For the true z coordinates, see the text.)

Table 11

Intensity Comparisons for Th_7M_3: (hk0) Data

Indices	Calc.	Obs.	Indices	Calc.	Obs.
100	0	0	440	22	10
110	0	0	530	58 ⎤	
200	0	0	700	28 ⎦	15
210	281	80	620	838	100
300	180	60	710	1640	140
220	660	100	540	248	40
310	34	0	630	177	15
400	44	20	800	41	15
320	32	10	720	7	5
410	85	15	810	37	10
500	767	60	550	2610	160
330	2010	160	640	12	0
420	31	0	730	42	0
510	27	10	900	1190	90
600	24	5	820	111	10
430	121	30	650	263 ⎤	
520	165	60	910	786 ⎦	70
610	97.4	30	740	412	20

Table 12

Intensity Comparisons for Th_7M_3: (hkl) Data

Indices	Calc.	Obs.	Indices	Calc.	Obs.
101	3	0	441	0	0
111	0	0	531	112 ⎤	248
201	17	47	701	22 ⎦	
211	320	341	621	628	561
301	231	282	711	15	0
221	0	0	541	220	213
311	21	73	631	284	144
401	64	83	801	241	75
321	108	53	721	38	82
411	87	74	811	173	26
501	323	424	551	0	0
331	0	0	641	40	54
421	10	0	731	1116	360
511	43	83	901	23	0
601	189	127	821	712	164
431	83	130	651	714 ⎤	470
521	191	217	911	73 ⎦	
611	95	101			

Table 13

Intensity Comparisons for Th$_7$ M$_3$: (hk2) Data

Indices	Calc.	Obs.	Indices	Calc.	Obs.
102	407	227	442	6	0
112	39	33	532	406 ⎤	
202	237	188	702	42 ⎦	640
212	29	31	622	18	29
302	20	22	712	38	70
222	5		542	41	54
312	10		632	23	24
402	19	30	802	363	507
322	452	583	722	234	298
412	44	69	812	33	74
502	26	32	552	103	121
332	47	57	642	199	344
422	93	126	732	121	159
512	140	159	902	65	62
602	1	0	822	1380	2083
432	82	122	652	730	212
522	44	121	912	174	101
612	2	0			

Table 14

Interatomic Distances in $Th_7 Fe_3$
(in Angstroms)

Atom	Neighbors		Distance	Bond Number
Th_I	2	Fe	2.89	.76
	2	Fe	2.90	.73
	2	Th_{II}	3.55	.39
	2	Th_I	3.72	.20
	4	Th_I	3.80	.15
Th_{II}	2	Fe	2.91	.70
	2	Th_{II}	3.43	.62
	2	Th_I	3.55	.39
	1	Th_{III}	3.60	.34
	1	Th_{III}	3.70	.22
	2	Th	3.76	.17
Th_{III}	3	Fe	2.96	.58
	3	Th_{II}	3.60	.34
	3	Th_{II}	3.70	.22
Fe	2	Th_I	2.89	.76
	1	Th_I	2.90	.73
	2	Th_{II}	2.91	.70
	1	Th_{III}	2.96	.58

Application of the zone theory

The number of bonding electrons in the unit cell of the Th_7M_3 compounds is 90.7 using Pauling's valences, 56 using Hume-Rothery's values, and 84 for the observed values using Pauling's radii. The radii of the spheres which will just contain these numbers of electrons are 2.47 $\underline{a}*$, 2.17 $\underline{a}*$, and 2.40 $\underline{a}*$, respectively. Some of the important planes in this structure are the $(\overline{2}20)$, (500), (330), (620), (710), (550), (900), (211), (301), (501), (621), (731), (102), (202), (322), (532), (802), (652), and (004) planes. The normal distance from the origin to one of these planes corresponds to the radius of a sphere which would be inscribed in a zone bounded by these planes. Only the normal to the (500) boundary plane, with the length 2.5 $\underline{a}*$, corresponds to the required size of the spheres.

The volumes of a few possible zones have been calculated. The zones bounded by (220) and (004) can contain 96 electrons. The zones bounded by the (202) planes can hold 93.3 electrons. The volumes of other simple zones which have been calculated are not at all suitable.

Conclusions

1. The structure of the Th_7M_3 compounds, where M is Fe, Co, or Ni, has been determined.

2. The structure has been considered from the viewpoint of the theories of metals. Pauling's suggestions concerning the valence and metallic radii seem to be consistent with this structure.

Summary

The unit cell dimensions and structure of the isostructural compounds, Th_7Fe_3, Th_7Co_3, and Th_7Ni_3, have been determined. The dimensions of the hexagonal unit cell of Th_7Fe_3 are $\underline{a} = 9.85$ A., $\underline{c} = 6.15$ A.; of Th_7Co_3 $\underline{a} = 9.83$ A., $\underline{c} = 6.17$ A.; of Th_7Ni_3 $\underline{a} = 9.86$ A., $\underline{c} = 6.23$ A. The atomic positions may be described on the basis of positions of space group C_{6v}^4 with the atoms in the following positions:

6 Th_I at $x, 2x, z$; $2\overline{x}, \overline{x}, z$; $x, \overline{x}, z$; $\overline{x}, x, \frac{1}{2} + z$; $\overline{x}, 2\overline{x}, \frac{1}{2} + z$; $2x, x, \frac{1}{2} + z$; with $\underline{x} = 0.126$ and $\underline{z} = 0.250$.

6 Th_{II} at the same positions with $\underline{x}$ = 0.544 and $\underline{z}$ = 0.03,
6 M at the same positions with $\underline{x}$ = 0.815 and $\underline{z}$ = 0.31,
2 Th_{III} at 1/3 2/3,z; 2/3,1/3,1/2+z; with $\underline{z}$ = $\overline{0}$.06.

The structure is discussed from the viewpoint of the theory of metals.

THE STRUCTURES OF U_2O_5 AND U_3O_8

Introduction

Early in the history of the X-ray diffraction method, Goldschmidt and Thomassen (19) investigated the minerals which had been found to con-tain uranium. As a result of these X-ray diffraction studies, they were able to report characteristic X-ray diagrams for UO_2 and U_3O_8. They found, however, that UO_3, prepared by oxidation of the minerals or by decomposition of uranyl nitrate, produced such broad diffraction maxima that they considered UO_3 amorphous. Goldschmidt and Thomassen reported that UO_2 was isostructural with the CaF_2 structure. The unit cell dimen-sions of the face-centered cubic unit for oxides obtained from several mineral sources ranged from 5.45 to 5.48 A. Van Arkel (20) later reported a value of 5.49 A. and Schoep and Billiet (21) found the unit cell dimen-sions to be 5.48 A. Neither the unit cell nor the structure of U_3O_8 or UO_3 was reported by any of these investigators.

The vapor pressure of oxygen in equilibrium with the uranium oxides and the density of the oxides throughout the range from UO_2 to UO_3 were studied thoroughly by Biltz and Müller (22). They found that the UO_2 phase extended up to about $UO_{2.25}$. Another one phase area extended from $UO_{2.62}$ to UO_3. The lower limit of this latter region depended upon the temperature at which the vapor pressure studies were made. UO_3 and U_3O_8 had equilibrium pressures of oxygen in the neighborhood of an atmosphere at 1100° C.; the vapor pressure, however, fell rapidly to a constant value of only a few millimeters at $UO_{2.62}$. Biltz and Müller confirmed the results of their vapor pressure studies by X-ray diagrams, but they did not report any structural determination of the U_3O_8 to UO_3 phase.

Lyden (23) heated U_3O_8, $KHCO_3$, and water in a sealed system. The oxide residue which resulted was found to have the composition U_2O_5. He also did not report any X-ray data.

No further work was performed on the uranium-oxygen system until the Manhattan Project demanded a complete knowledge of the chemistry of uranium. The uranium-oxygen system was again investigated using the X-ray diffraction method. Pederagani and Rosenbaum (24) reported more precise values of the unit cell dimensions of UO_2 as $a = 5.4678 \pm .0005$ A. Rundle et al. (25) reported almost identical unit cell dimensions ($a = 5.4691 \pm .0005$ A.). Zachariasen (26) reported unit cell dimensions and possible structures for several crystalline forms of UO_3 and a pseudo unit cell for U_3O_8. He also demonstrated a possible relationship between the U_3O_8 and the UO_3 structures.

The region between UO_2 and UO_3 was also investigated by the X-ray diffraction method by Rundle et al. (25). The uranium oxide samples in this region were prepared by mixing appropriate amounts of UO_2 and U_3O_8 or U_3O_8 and UO_3 and heating them in sealed quartz tubes until equilibrium had been attained. The X-ray diagrams from these samples confirmed the solubility of oxygen in uranium dioxide up to approximately $UO_{2.25}$ as noted by Biltz and Müller. Samples with larger amounts of oxygen contained a new phase. The positions of the lines of the new phase in the diffraction diagrams changed gradually to those characteristic of U_3O_8 and then to those of UO_3 as samples with increasing oxygen content were examined. It was obvious from the diffraction diagrams that the U_3O_8 structure was not the limiting structure of the one phase area but only one occurring in the transition from the limiting structure to UO_3. In this investigation the pseudo cell of U_3O_8 found by Zachariasen was also confirmed. In addition, the true unit cell, based on the pseudo unit, was determined by powder diagrams.

Recently, Grönvold (27) has reported the results of oxidation studies made on UO_2. He also has confirmed the solubility of oxygen in UO_2 up to $UO_{2.34}$, and has found that the density increases in accordance with the results of Biltz and Müller. A tetragonal phase, closely related to UO_2 was found for compositions between $UO_{2.34}$ and higher oxides. He also reported a pseudo unit cell for U_3O_8 and possible atomic positions which agree with those of Zachariasen. Jolibois (28) in oxidation studies of UO_2 has reported the preparation of U_3O_7 or $UO_{2.33}$, but does not report its structure.

The Determination of the Limit of the One Phase Area

It was noted that the UO_2 maxima occurred in powder diagrams of the oxide prepared by mixing an equal number of moles of UO_2 and U_3O_8 and

heating them to 1100° C. in a sealed system. The intensities of the UO_2 maxima were much weaker than those of the U_3O_8-like phase. In order to determine the relative amount of UO_2 which was present, a series of standard mixtures of UO_2 and U_3O_8 were prepared. These oxide mixtures were examined in the unfired condition. The sample with a ratio of eight moles of U_3O_8 to one mole of UO_2 produced an X-ray diagram in which the ratio of the line intensities of the UO_2 phase to those of the U_3O_8-like phase appeared to be the same as that from the mixture of overall composition U_2O_5. From the equation,

$$8 \ UO_x + UO_{2.25} = 9 \ UO_{2.5},$$
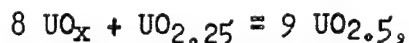
the composition of the U_3O_8-like phase was found to be $UO_{2.53}$. If the solubility limit of Grönvold is used,

$$8 \ UO_x + UO_{2.34} = 9 \ UO_{2.5},$$
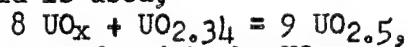
the composition of the phase is found to be $UO_{2.52}$.

This determination is subject to the limitation that the UO_x phase might have been coating the $UO_{2.25}$ phase and cutting down the intensity by absorption. On the other hand, the reaction between $UO_{2.25}$ and UO_x may not have been completed.

The Pseudo Unit Cells of $UO_{2.5}$, U_3O_8, and UO_3

Zachariasen (26) has reported a simple hexagonal unit cell for one form of UO_3. The unit cell dimensions are $a = 3.971 \pm .004$ A., $c = 4.168 \pm .008$ A. The uranium atoms are at the corners of the unit cell; the three oxygen atoms are at $(00\frac{1}{2})$ and $\pm(1/3, 2/3, u)$ with $u = 0.17$.

The UO_3 structure may also be described using an end-centered orthorhombic unit cell in which the ratio of the length of the a axis to the length of the b axis is $\sqrt{3}$. This relationship is shown in figure 4. This end-centered orthorhombic unit cell now has two uranium atoms per unit cell at (000) and $(\frac{1}{2}\frac{1}{2}0)$. The unit cell dimensions are given in table 15.

The pseudo unit cell of U_3O_8 reported by Zachariasen is also orthorhombic with dimensions very similar to the orthorhombic unit cell for UO_3. (See table 15). Again, the uranium atom positions are at (000) and $(\frac{1}{2}\frac{1}{2}0)$. The true unit cell dimensions for U_3O_8 result upon tripling the b axis of the pseudo unit. The relationship between this unit and that of UO_3 is shown in figure 5.

Table 15

Pseudo Unit Cell Dimensions of UO_3, U_3O_8 and U_2O_5
(in Angstroms)

Compound	a	b	c
UO_3	$6.878 \pm .007$	$3.971 \pm .004$	$4.168 \pm .008$
U_3O_8	6.71	3.99	4.15
U_2O_5	6.734	3.964	4.143

An effort was made to index the maxima in the powder diagrams of the U_2O_5 phase since the diagrams appeared similar to those of U_3O_8. Again, a pseudo unit cell was found which is orthorhombic; the dimensions are given in table 15. The weak maxima, however, could not be explained by tripling the b axis as for U_3O_8.

Preparation of U_2O_5 Single Crystals

Fortunately, the structure determination of U_2O_5 did not have to depend upon data from powder diagrams alone. As the result of decomposition of UO_2Cl_2 at 900° in a quartz vessel, a mixture of U_2O_5 and $UO_{2.25}$ was formed in which many single crystals of U_2O_5 could be found, as well as occasional crystals of $UO_{2.25}$. The single crystals were needle-like with a cross-section in the shape of a parallelogram with an obtuse angle of approximately 120°. Some of the needles were powdered and examined by the powder method. The diagrams from this material corresponded exactly with those of U_2O_5 made from UO_2 and U_3O_8 as described previously.

X-ray Diffraction Data

Experimental methods

Equipment. The powder diagrams were prepared in a powder camera of 5.73 cm. radius with the film mounted in the Straumanis fashion and in an unsymmetrical self-focussing powder camera with a 10 cm. radius. The latter camera possesses very high dispersion which enabled the complex powder diagrams of the U_3O_8-like phases to be interpreted. The single
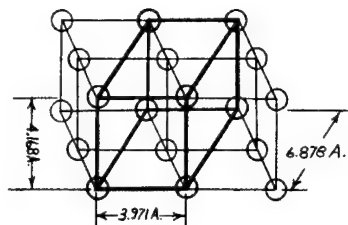
Fig. 4--The relationship of the orthorhombic
unit cell to the hexagonal unit cell of UO_3.
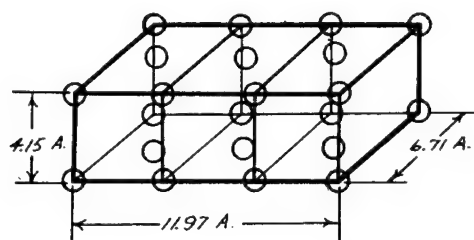
Fig. 5--Unit cell of U_3O_8.
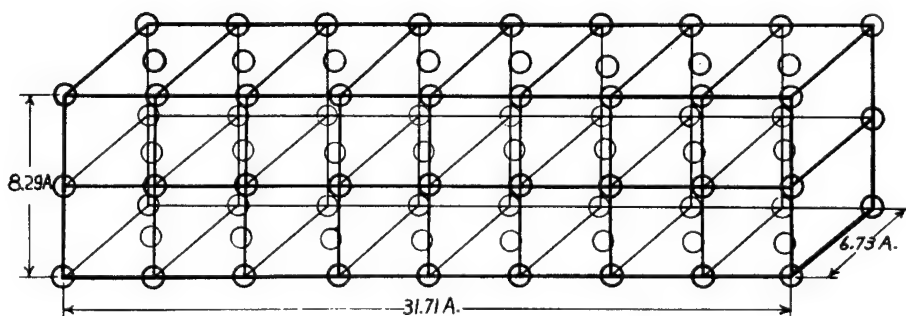
Fig. 6--Unit cell of U_2O_5.

crystal diagrams of U_2O_5 were prepared in a Weissenberg camera of 2.836 cm. radius.

Source of X-rays. Nickel filtered copper characteristic K radiation was used for the powder and single crystal investigations.

Intensity determination and correction. The intensities of the diffraction maxima were estimated visually from the Weissenberg diagrams. The intensity data were recorded using five films, each one mounted in back of the next one, for each exposure. By this arrangement a numerical scale of intensities dependent on the constant absorption of X-ray by the films was established upon which the estimation of intensities was based.

The F^2 values for use in the Patterson projections were found from the following formula,

$$F^2 \propto I/LPA,$$

where I is the intensity observed; L, the Lorentz factor; P, the polarization factor; A, the absorption factor; and F, the structure factor. The absorption factor for the (hk0) reflections (c = the needle axis) was taken to be that for a cylindrical rod with a diameter equal to the average diameter of the crystal (0.001 cm.). The experimental F values for use in the Fourier series are the square roots of the F^2 values found above.

The observed F(hk0) values which are used for comparison with the F(hk0) values in table 17 are the F values corrected as above with an additional correction for the temperature factor. The temperature factor was determined by plotting log $F_{obsd.}/F_{calcd.}$ versus $\sin^2\Theta$ and finding the slope of the straight line drawn through these points.

The intensities of the (0kℓ) reflections were calculated by use of the following formula:

$$I' \propto FF*LPA.$$

The logarithms of $I_{obsd.}/I'$ were then plotted versus $\sin^2\Theta$ to find an average temperature factor. The calculated intensities were then adjusted for this effect. The absorption factor for these reflections was by far the most important correction as the rotation axis was perpendicular to the needle axis. The integrals $\int e^{-\mu S} dV$ where μ is the linear absorption coefficient, and S is the length of path of the X-rays in the crystal in scattering from the elemental volume dV, were calculated for all reflections. In order to reduce the labor of calculation, the general forms of the integrals were first calculated and simplified by dropping all

terms which it appeared would be insignificant. For most of the reflec-
tions this approximation seems to be justified. A few of the reflections,
however, still are not adequately corrected. The absorption factor for
(0kℓ) reflections where $\underline{k}$ is less than sixteen apparently is still too
high.

Unit cell dimensions of U_2O_5

The single crystals of U_2O_5 were examined by the Weissenberg method.
Moving film diagrams were taken with the crystal rotating about the $\underline{a}$, $\underline{b}$,
and $\underline{c}$ axes. From the diagrams it was clear that the true unit cell
corresponded to doubling the pseudo cell's $\underline{c}$ axis and multiplying the
pseudo cell's $\underline{b}$ axis by eight. (See figure 6.) The true unit cell di-
mensions, calculated from the pseudo cell dimensions obtained from powder
diagrams, are, then, $\underline{a}$ = 6.73 $\pm$ .02 A., $\underline{b}$ = 31.71 $\pm$ .1 A., $\underline{c}$ = 8.29 $\pm$
.02 A. (The description of the axes has been changed from that in ref-
erence 25 to show the relationship to the hexagonal unit cell of UO_3.)

The X-ray density calculated with thirty-two uranium atoms and
consequently eighty oxygen atoms per unit cell is 8.35 g/cc. Biltz and
Müller (22) found a value of 8.78 g/cc. for the density of samples in
this region and a value of 8.37 for samples with a composition $UO_{2.64}$.
Their density values, however, were so widely scattered and so dependent
upon the method of preparation of the samples, that little reliance can
be placed upon their results.

Structural Determination

The determination of the space group

All reflections from U_2O_5 which were observed may be classed in the
following manner:

(hkℓ) present in all orders,
(0kℓ) present only if $\underline{k}$ is even,
(hk0) present in all orders,
($\underline{h}$0ℓ) present only if $\underline{h}$ is even, ℓ is even,
($\underline{h}$00) present only if $\overline{h}$ is even,
($\overline{0k}$0) present only if $\overline{k}$ is even,
(00ℓ) present only if $\overline{\ell}$ is even.

The $(hk\ell)$ data require a primitive unit cell. The $(0k\ell)$ data indicate the presence of a "b" glide plane perpendicular to $\underline{a}$; the $(h0\ell)$ data indicate either an "a", "c" or "n" glide plane perpendicular to $\underline{b}$. No glide planes are indicated perpendicular to $\underline{c}$. The $(h00)$, $(0k0)$ and (00ℓ) data indicate possible two-fold screw axes along $\underline{a}$, $\underline{b}$, and $\underline{c}$ respectively. Since the same extinctions are required by the glide planes along these same axes, the presence of screw axes is indeterminate.

On the basis of these symmetry elements, it is possible to eliminate all of the fifty-nine orthorhombic space groups except the following:

D_{2h}^{16} – Pnma	D_2^4 – $P2_12_12_1$	C_{2v}^9 – Pna
D_{2h}^{13} – Pmmn	D_2^3 – $P2_12_12$	C_{2v}^8 – Pba
D_{2h}^{11} – Pbcm	D_2^2 – $P2_122$	C_{2v}^7 – Pmn
D_{2h}^9 – Pbam	D_2^1 – $P222$	C_{2v}^5 – Pca
D_{2h}^5 – Pmma		C_{2v}^4 – Pma
D_{2h}^1 – Pmmm		C_{2v}^2 – Pmc
		C_{2v}^1 – Pmm

The reflections which correspond to the pseudo unit cell are very strong; the reflections requiring the larger unit cell are weak. The intensities of the reflections requiring the larger unit cell, after correction for all angle-dependent factors except the temperature factor, become stronger in the back reflection region and approach the magnitude of the pseudo cell reflections. Therefore, it has been assumed that the intensities of these reflections are due primarily to uranium atoms. Thus, in order to produce the strong reflections, the uranium atoms must be very close to the positions which they would occupy in an ideal unit cell built from pseudo cell units. The weaker reflections arise due to slight distortions from these ideal positions. The uranium atoms positions in this ideal cell are obtained by adding 000 and $00\frac{1}{2}$ to

$$\pm \begin{bmatrix} 1/2,1/16,0; & 1/2,3/16,0; & 1/2,5/16,0; & 1/2,7/16,0; \\ 0,1/8,0; & 0,3/8,0; & 0,1/4,0; & 0,1/2,0; & 0,0,0; \end{bmatrix}$$

All the space groups listed above permit the uranium atoms to be arranged in the ideal fashion. Some of them, however, allow the uranium atoms to be in eight-fold positions; others allow only four-fold positions

to be used. A list of positions available in the space groups is given in table 16. Only the general positions are listed and the axes have been transformed from those in the "Internationale Tabellen fur Bestimmung von Kristrallstrukturen" (29) to agree with the choice of axes already made.

These positions may be subdivided by considering only the positions in the (x,y) plane. The positions then resolve into those designated by A, B, C etc. There are only five types of eight-fold positions. Of these five types, three, B, D, E, reduce to four-fold positions before being applicable to this structure. For each value of y, there are four positions given in these eight-fold sets, whereas the "ideal" structure calls for only two such positions. These positions as well as all of the other four-fold positions available in the lower space groups do not need to be considered unless the eight-fold positions remaining fail to provide a suitable structure.

The determination of the x and y parameters

The "ideal" x and y parameters for the eight-fold positions A are

x	y
1/4	1/32
3/4	3/32
1/4	5/32
3/4	7/32

and for positions C

x	y
1/2	1/16
0	1/8
1/2	3/16
0	1/4

and 0 1/2 (four-fold positions).
(Parameterless four-fold positions are available in D_{2h}^{11}.)

A Patterson F^2 projection was made using $(0\underline{k}0)$ data by evaluating the formula,

$$p(\underline{y}) = \sum_{\underline{K}} F^2 (0\underline{k}0) e^{2\pi i\underline{k}\underline{y}} .$$

From this projection it appeared that the parameters would be shifted

from 0.125 to 0.122 or 0.128, from 0.0625 to 0.065 or 0.060, and from 0.1875 to 0.190 or 0.185 for positions C. By trial and error the combination 0.060, 0.128, and 0.185 or 0.065, 0.122 and 0.190 together with the parameterless y positions were found to explain the intensities of the (0k0) reflections. A Fourier projection was made using the observed $\bar{F}_{(0k0)}$ data and the signs determined by calculation on the basis of the positions above. The evaluation of the formula, $\rho(y) = \sum_K F_{(0k0)} e^{-2\pi iky}$, led to the parameter values 0.060, 0.129 and 0.184.

A Patterson projection using (hk0) data according to the formula, $p(x,y) = \sum_h \sum_K F^2 (hk0) e^{2\pi i(hx + ky)}$, gave peaks at the points expected if the atoms were in their "ideal" positions. The peaks at 1/16, 1/8, and 1/4 of b extended in the x direction, however.

By trial and error it was found that a suitable combination of the parameters would be the following:

x	y
0.53	0.060
0.98	0.129
0.50	0.184
0.03	0.250

together with the parameterless four-fold position. These values were used in calculating F values for the (hk0) reflections. The signs of the calculated F's were used with the observed F's in carrying out a Fourier summation of the data. The values of the x and y parameters found by this method are:

x	y
0.539	0.0591
0.988	0.1295
0.505	0.1841
0.047	0.2500
0.000	0.0000.

Possible values for the (x,y) parameters were found for the eight-fold positions, A, by trial and error. Again, a Fourier projection along a line was made using (0k0) data. The parameters obtained in this manner, 0.036, 0.092, 0.154 and 0.222, were used in a further trial and error procedure to determine the x parameters. The approximate sets of x and y parameters which were found to give rough agreement with the

Table 16

General Positions Available for the U_2O_5 Structure

Space group		Positions
D_{2h}^{16}	A	$xyz;\quad \overline{x},\overline{y},\frac{1}{2}+z;\quad \frac{1}{2}+x,\frac{1}{2}-y,\overline{z};\quad \frac{1}{2}-x,\frac{1}{2}+y,\frac{1}{2}-z;\quad x,y,\frac{1}{2}-z;$ $\overline{x},\overline{y},\overline{z};\quad \frac{1}{2}+x,\frac{1}{2}-y,\frac{1}{2}+z;\quad \frac{1}{2}-x,\frac{1}{2}+y,z;$
D_{2h}^{13}	B	$xyz;\quad \overline{x}\overline{y}\overline{z};\quad \overline{x}y z;\quad xy\overline{z};\quad \frac{1}{2}+x,\overline{y},\frac{1}{2}+z;\quad \frac{1}{2}-x,\overline{y},\frac{1}{2}-z;\quad \frac{1}{2}+x,\overline{y},\frac{1}{2}-z;$ $\frac{1}{2}-x,\overline{y},\frac{1}{2}+z;$
D_{2h}^{11}	C	$xyz;\quad \overline{x}\overline{y}\overline{z};\quad \overline{x},\overline{y},\frac{1}{2}+z;\quad x,y,\frac{1}{2}-z;\quad x,\frac{1}{2}-y,\overline{z};\quad \overline{x},\frac{1}{2}+y,\frac{1}{2}-z;$ $x,\frac{1}{2}-y,\frac{1}{2}+z;\quad \overline{x},\frac{1}{2}+y,z;$
D_{2h}^{9}	A	$xyz;\quad \overline{x}\overline{y}z;\quad xy\overline{z};\quad \overline{x}\overline{y}\overline{z};\quad \frac{1}{2}+x,\frac{1}{2}-y,\overline{z};\quad \frac{1}{2}-x,\frac{1}{2}+y,\overline{z};\quad \frac{1}{2}+x,\frac{1}{2}-y,z;$ $\frac{1}{2}-x,\frac{1}{2}+y,z;$
D_{2h}^{5}	D	$xyz;\quad \overline{x}\overline{y}\overline{z};\quad xy\overline{z};\quad \overline{x}\overline{y}z;\quad \frac{1}{2}+x,\overline{y},\overline{z};\quad \frac{1}{2}-x,y,z;\quad \frac{1}{2}+x,\overline{y},z;$ $\frac{1}{2}-x,y,\overline{z};$
	C	$xyz;\quad \overline{x}\overline{y}z;\quad xy\overline{z};\quad \overline{x}\overline{y}z;\quad x,\frac{1}{2}-y,z;\quad \overline{x},\frac{1}{2}+y,\overline{z};\quad x,\frac{1}{2}-y,\overline{z};$ $\overline{x},\frac{1}{2}+y,z;$
	E	$xyz;\quad \overline{x}\overline{y}z;\quad x\overline{y}z;\quad \overline{x}yz;\quad x,y,\frac{1}{2}-z;\quad \overline{x},\overline{y},\frac{1}{2}+z;\quad x,\overline{y},\frac{1}{2}+z;$ $\overline{x},y,\frac{1}{2}-z;$
D_{2h}^{1}	E	$xyz;\quad \overline{x}\overline{y}z;\quad x\overline{y}\overline{z},\quad \overline{x}y\overline{z};\quad xy\overline{z};\quad \overline{x}\overline{y}\overline{z};\quad x\overline{y}z;\quad \overline{x}yz;$
D_{2}^{4}	F	$xyz;\quad \frac{1}{2}+x,\frac{1}{2}-y,\overline{z};\quad \frac{1}{2}-x,\overline{y},\frac{1}{2}+z;\quad \overline{x},\frac{1}{2}+y,\frac{1}{2}-z;$
	G	$xyz;\quad \frac{1}{2}+x,\overline{y},\frac{1}{2}-z;\quad \frac{1}{2}-x,\frac{1}{2}+y,\overline{z};\quad \overline{x},\frac{1}{2}-y,\frac{1}{2}+z;$
D_{2}^{3}	A	$xyz;\quad \overline{x}\overline{y}z;\quad \frac{1}{2}+x,\frac{1}{2}-y,\overline{z};\quad \frac{1}{2}-x,\frac{1}{2}+y,\overline{z};$
	B	$xyz;\quad \overline{x}y\overline{z};\quad \frac{1}{2}+x,\overline{y},\frac{1}{2}-z;\quad \frac{1}{2}-x,\overline{y},\frac{1}{2}+z;$
	H	$xyz;\quad x\overline{y}\overline{z};\quad \overline{x},\frac{1}{2}+y,\frac{1}{2}+z;\quad \overline{x},\frac{1}{2}-y,\frac{1}{2}-z;$
D_{2}^{2}	E	$xyz;\quad \overline{x},\overline{y},\frac{1}{2}+z;\quad x\overline{y}\overline{z};\quad \overline{x},y,\frac{1}{2}-z;$

Table 16

(Continued)

Space group		Positions		
	E	$xyz;$	$\overline{x},\overline{y},\frac{1}{2}+z,$ $\overline{xy}\overline{z};$	$x,\overline{y},\frac{1}{2}-z;$
	D	$xyz;$	$\overline{xy}z;$	$\frac{1}{2}+x,\overline{y},\overline{z};$ $\frac{1}{2}-x,y,\overline{z};$
	B	$xyz;$	$\overline{x}yz;$	$\frac{1}{2}+x,\overline{y},\overline{z};$ $\frac{1}{2}-x,\overline{y},z;$
D_2^2	H	$xyz;$	$x\overline{y}\overline{z};$	$\overline{x},\frac{1}{2}+y,\overline{z};$ $\overline{x},\frac{1}{2}-y,z;$
	C	$xyz;$	$\overline{xy}z;$	$x,\frac{1}{2}-y,\overline{z};$ $\overline{x},\frac{1}{2}+y,\overline{z};$
D_2^1	E	$xyz;$	$\overline{xy}z;$	$x\overline{yz};$ $\overline{x}y\overline{z};$
C_{2v}^9	A	$xyz;$	$\overline{x},\overline{y},\frac{1}{2}+z;$	$\frac{1}{2}+x,\frac{1}{2}-y,\frac{1}{2}+z;$ $\frac{1}{2}-x,\frac{1}{2}+y,z;$
C_{2v}^8	A	$xyz;$	$\overline{xy}z;$	$\frac{1}{2}+x,\frac{1}{2}-y,z;$ $\frac{1}{2}-x,\frac{1}{2}+y,z;$
C_{2v}^7	B	$xyz;$	$\overline{x}yz;$	$\frac{1}{2}+x,\overline{y},\frac{1}{2}+z;$ $\frac{1}{2}-x,\overline{y},\frac{1}{2}+z;$
	I	$xyz;$	$xy\overline{z};$	$\frac{1}{2}+x,\overline{y},\frac{1}{2}-z;$ $\frac{1}{2}+x,\overline{y},\frac{1}{2}+z;$
C_{2v}^5	C	$xyz;$	$\overline{x},\overline{y},\frac{1}{2}+z;$	$x,\frac{1}{2}-y,\frac{1}{2}+z;$ $x,\frac{1}{2}+y,z;$
C_{2v}^4	D	$xyz;$	$\overline{xy}z;$	$\frac{1}{2}+x,\overline{y},z;$ $\frac{1}{2}-x,y,z;$
	C	$xyz;$	$\overline{xy}z;$	$x,\frac{1}{2}-y,z;$ $\overline{x},\frac{1}{2}+y,z;$
	J	$xyz;$	$x\overline{yz};$	$x,\frac{1}{2}-y,z;$ $x,\frac{1}{2}+y,\overline{z};$
	K	$xyz;$	$\overline{xyz};$	$\frac{1}{2}-x,y,z;$ $\frac{1}{2}+x,y,\overline{z};$
	L	$xyz;$	$x\overline{yz};$	$x,y,\frac{1}{2}-z;$ $x,\overline{y},\frac{1}{2}+z;$
	M	$xyz;$	$\overline{xy}\overline{z};$	$x,y,\frac{1}{2}-z;$ $\overline{x},y,\frac{1}{2}+z;$

Table 16

(Continued)

Space group		Positions			
C_{2v}^2	E	xyz;	$\overline{x},\overline{y},\frac{1}{2}+z$;	$x,\overline{y},\frac{1}{2}+z$;	$\overline{x}yz$;
	E	xyz;	$x\overline{yz}$;	$\overline{x},\overline{y},\frac{1}{2}+z$;	$\overline{x},y,\frac{1}{2}+z$;
	N	xyz;	$\overline{xyz}$;	$x,\frac{1}{2}+y,\overline{z}$;	$\overline{x},\frac{1}{2}+y,\overline{z}$;
	I	xyz;	$xy\overline{z}$;	$\frac{1}{2}+x,\overline{y},z$;	$\frac{1}{2}+x,\overline{y},\overline{z}$;
	O	xyz;	$xy\overline{z}$;	$\overline{x},\frac{1}{2}+y,\overline{z}$;	$x,\frac{1}{2}+y,z$;
C_{2v}^1	E	xyz;	$\overline{xyz}$;	$x\overline{yz}$;	$\overline{x}yz$;

observed amplitudes were the following:

x	y
0.270	0.036
0.750	0.092
0.220	0.154
0.750	0.222

An electron density map was again prepared using the signs as determined from this approximate arrangement together with the observed amplitudes as coefficients of the Fourier series. The new parameters, which were determined from the peaks in the electron density map, did not differ markedly from the above values. The new parameters are listed below:

x	y
0.2825	0.0352
0.745	0.092
0.2067	0.1546
0.745	0.2227

The two sets of calculated F values together with the observed values are shown in table 17. There seems to be little difference between the agreement of either set with the observed values. The close similarity of the absolute values of the F values is more easily understood if the relationship between the structures is demonstrated. If one adds 0.250 to the $\underline{x}$ and 0.4062 to the $\underline{y}$ values of the coordinates of the atoms in the structure based on positions A, the coordinates will become almost identical to the coordinates of the atoms in the structure based on positions C. This relationship is demonstrated in table 18. Projections of the arrangements on the (x,y) plane are shown in figures 7 and 8.

The determination of the z parameters

The determination of the $\underline{z}$ parameters is difficult because of the uncertainty introduced by the absorption factor. Assuming, however, that either arrangement A or C is possible for the (x,y) plane, there are only two sets of (y,z) positions available in the eight-fold positions. The positions are listed below.

D_{2h}^{16} A $y,z;\quad \bar{y},\tfrac{1}{2}+z;\quad \tfrac{1}{2}-y,z;\quad \tfrac{1}{2}+y,\tfrac{1}{2}-z;$
$\qquad\qquad \bar{y},\bar{z};\quad y,\tfrac{1}{2}-z;\quad \tfrac{1}{2}+y,\bar{z};\quad \tfrac{1}{2}-y,\tfrac{1}{2}+z;$

D_{2h}^{11} C Same positions as above

D_{2h}^{9} A $y,z;\quad y,\bar{z};\quad \tfrac{1}{2}+y,\bar{z};\quad \tfrac{1}{2}+y,z;$
$\qquad\qquad \bar{y},\bar{z};\quad \bar{y},z;\quad \tfrac{1}{2}-y,z;\quad \tfrac{1}{2}-y,z;$

D_{2h}^{5} C Same positions as above.

The first set of positions requires that the ideal parameter value of $\underline{z}$ must be zero or one-half. The second set requires the ideal parameter values to be one-quarter or three-quarters. The decision among the four possible arrangements was made on the basis of a systematic trial and error procedure to determine the parameters. Parameters could be found for arrangements in D_{2h}^{16} and D_{2h}^{5} which would satisfy the intensity data. The values of the parameters which were used in the intensity comparisons in table 19 are listed below.

D_{2h}^{16}		D_{2h}^{5}	
y	z	y	z
0.0345	0.013	0.0592	0.259
0.0915	0.993	0.129	0.244
0.1546	0.995	0.1841	0.238
0.2227	0.016	0.2500	0.265
		0.0000	0.220

Table 17

Amplitude Comparisons for U_2O_5: (hk0) Data

Indices	Calculated F		Observed F
	Positions A	Positions C	
010	0	0	0
020	0	1	0
030	0	0	0
040	2	1	0
050	0	0	0
060	26	27	15
070	0	0	0
080	1	1	0
090	0	0	0
0,10,0	41	41	22
0,11,0	0	0	0
0,12,0	4	4	0
0,13,0	0	0	0
0,14,0	1	4	0
0,15,0	0	0	0
0,16,0	259	260	180
0,17,0	0	0	0
0,18,0	1	5	0
0,19,0	0	0	0
0,20,0	9	8	0
0,21,0	0	0	0
0,22,0	68	70	54
0,23,0	0	0	0
0,24,0	1	3	0
0,25,0	0	0	0
0,26,0	74	75	68
0,27,0	0	0	0

Table 17

(Continued)

| Indices | Calculated F | | Observed F |
	Positions A	Positions C	
0,28,0	15	14	0
0,29,0	0	0	0
0,30,0	4	8	0
0,31,0	0	0	0
0,32,0	164	164	173
0,33,0	0	0	0
0,34,0	4	8	6
0,35,0	0	0	0
0,36,0	20	18	0
0,37,0	0	0	0
0,38,0	82	84	65
0,39,0	0	0	0
0,40,0	1	8	0
100	0	1	0
110	10	3	0
120	4	6	0
130	37	33	36
140	1	2	0
150	6	1	0
160	1	2	0
170	21	14	0
180	300	301	218
190	11	11	0
1,10,0	0	2	0
1,11,0	9	0	0
1,12,0	2	1	0
1,13,0	34	31	58
1,14,0	1	4	0

Table 17

(Continued)

| Indices | Calculated F | | Observed F |
	Positions A	Positions C	
1,15,0	12	5	0
1,16,0	1	2	0
1,17,0	2	2	0
1,18,0	58	58	62
1,19,0	24	21	0
1,20,0	9	7	0
1,21,0	1	0	0
1,22,0	2	5	0
1,23,0	23	19	0
1,24,0	203	201	187
1,25,0	2	11	0
1,26,0	2	6	0
1,27,0	9	0	0
1,28,0	10	11	0
1,29,0	24	22	18
1,30,0	77	78	83
1,31,0	8	5	0
1,32,0	0	6	0
1,33,0	4	6	0
1,34,0	77	77	70
1,35,0	14	11	0
1,36,0	21	18	0
1,37,0	0	1	0
1,38,0	51	7	0
1,39,0	11	18	0
1,40,0	129	128	166
200	291	293	218
210	32	19	43

Table 17

(Continued)

| Indices | Calculated F | | Observed F |
	Positions A	Positions C	
220	2	1	0
230	9	2	0
240	2	5	0
250	59	61	50
260	35	36	34
270	16	8	0
280	0	1	0
290	1	1	0
2,10,0	25	26	58
2,11,0	49	60	57
2,12,0	2	1	0
2,13,0	3	1	0
2,14,0	1	2	0
2,15,0	41	38	49
2,16,0	234	236	214
2,17,0	14	12	0
2,18,0	0	4	0
2,19,0	9	1	0
2,20,0	2	1	0
2,21,0	49	50	47
2,22,0	72	74	61
2,23,0	15	10	0
2,24,0	0	4	0
2,25,0	4	24	0
2,26,0	60	62	70
2,27,0	35	30	38
2,28,0	15	12	0
2,29,0	1	2	0

Table 17

(Continued)

Indices	Calculated F		Observed F
	Positions A	Positions C	
2,30,0	3	5	0
2,31,0	72	36	45
2,32,0	152	151	164
2,33,0	2	0	0
2,34,0	3	7	0
2,35,0	6	2	0
2,36,0	13	11	0
2,37,0	36	37	31
2,38,0	80	85	72
2,39,0	13	9	0
2,40,0	1	7	0
300	0	4	0
310	16	8	0
320	19	16	0
330	76	77	97
340	5	1	0
350	10	1	0
360	3	1	0
370	51	46	59
380	235	233	186
390	30	27	49
3,10,0	7	1	0
3,11,0	14	1	0
3,12,0	7	10	0
3,13,0	74	77	63
3,14,0	65	64	66
3,15,0	24	15	0
3,16,0	0	4	0

Table 17

(Continued)

| Indices | Calculated F | | Observed F |
	Positions A	Positions C	
3,17,0	2	3	0
3,18,0	31	30	37
3,19,0	54	53	67
3,20,0	9	5	0
3,21,0	1	1	0
3,22,0	2	2	0
3,23,0	56	50	50
3,24,0	170	171	190
3,25,0	9	30	0
3,26,0	1	4	0
3,27,0	11	1	0
3,28,0	1	2	0
3,29,0	58	59	64
3,30,0	82	83	62
3,31,0	20	13	30
3,32,0	1	6	0
3,33,0	11	4	0
3,34,0	55	57	64
3,35,0	33	31	36
3,36,0	23	18	0
3,37,0	5	4	0
3,38,0	2	1	0
400	201	207	165
410	44	42	44
420	5	1	0
430	14	13	0
440	11	16	0

Table 17

(Continued)

Indices	Calculated F		Observed F
	Positions A	Positions C	
450	88	90	80
460	54	54	66
470	27	18	0
480	1	6	0
490	14	6	0
4,10,0	9	5	0
4,11,0	73	76	60
4,12,0	1	5	0
4,13,0	6	1	0
4,14,0	2	1	0
4,15,0	66	57	54
4,16,0	170	176	141
4,17,0	22	15	37
4,18,0	4	0	0
4,19,0	16	2	0
4,20,0	12	16	0
4,21,0	89	80	71
4,22,0	80	81	70
4,23,0	29	19	0
4,24,0	1	11	0
4,25,0	5	38	0
4,26,0	27	31	36
4,27,0	49	51	50
4,28,0	16	11	0
4,29,0	3	4	0
4,30,0	24	2	0
4,31,0	66	61	51
4,32,0	118	120	119

Table 17

(Continued)

Indices	Calculated F		Observed F
	Positions A	Positions C	
4,33,0	3	2	0
4,34,0	15	3	0
4,35,0	10	1	0
4,36,0	14	7	0
500	0	8	0
510	24	16	0
520	48	45	47
530	87	90	74
540	9	17	0
550	12	0	0
560	6	1	0
570	41	51	69
580	154	161	136
590	37	28	54
5,10,0	7	2	0
5,11,0	18	1	0
5,12,0	19	25	0
5,13,0	88	92	72
5,14,0	78	77	70
5,15,0	33	23	0
5,16,0	2	7	0
5,17,0	6	2	0
5,18,0	7	4	0
5,19,0	66	65	69
5,20,0	8	1	0
5,21,0	0	4	0
5,22,0	2	4	0
5,23,0	72	63	64
5,24,0	119	124	117

Table 17

(Continued)

Indices	Calculated F		Observed F
	Positions A	Positions C	
5,25,0	11	40	23
5,26,0	4	1	0
5,27,0	16	1	0
5,28,0	19	22	0
5,29,0	72	89	75
5,30,0	88	91	77
5,31,0	31	21	0
5,32,0	2	6	0
5,33,0	12	12	0
600	120	126	123
610	48	37	57
620	10	3	0
630	17	1	0
640	19	27	0
650	87	92	70
660	74	73	70
670	34	23	0
680	3	10	0
690	3	14	0
6,10,0	43	40	22
6,11,0	75	76	75
6,12,0	2	9	0
6,13,0	6	3	0
6,14,0	5	4	0
6,15,0	68	57	66
6,16,0	107	116	141
6,17,0	21	12	17

Table 17

(Continued)

Indices	Calculated F		Observed F
	Positions A	Positions C	
6,18,0	9	4	0
6,19,0	20	3	0
6,20,0	27	32	0
6,21,0	79	85	78
6,22,0	48	90	74
6,23,0	37	25	0
6,24,0	4	8	0
6,25,0	1	43	0
6,26,0	12	6	0
6,27,0	55	52	57
6,28,0	17	10	0
6,29,0	6	7	0
700	0	3	0
710	31	24	0
720	51	69	64
730	76	80	60
740	12	22	0
750	14	2	0
760	11	0	0
770	56	43	60
780	80	96	101
790	31	19	42
7,10,0	13	6	0
7,11,0	22	2	0
7,12,0	29	37	15
7,13,0	47	85	78
7,14,0	89	89	74

Table 17

(Continued)

Indices	Calculated F		Observed F
	Positions A	Positions C	
7,15,0	40	30	0
7,16,0	5	12	0
7,17,0	14	12	0
7,18,0	43	37	12
7,19,0	61	61	56
7,20,0	10	0	0
7,21,0	0	6	0
7,22,0	5	9	0
7,23,0	72	60	48
7,24,0	70	77	96
800	62	74	81
810	39	23	43
820	17	6	0
830	18	0	0
840	22	33	0
850	68	75	66
860	88	88	62
870	40	32	0
880	3	15	0
890	27	25	0
8,10,0	70	17	57
8,11,0	60	63	56
8,12,0	0	11	0
8,13,0	5	7	0
8,14,0	11	4	0

Table 18

Relationship between Structures Based on A and C

Positions A*		Positions C		Deviation	
x	y	x	y	x	y
0.532	0.4414	0.539	0.4409	0.007	0.0005
0.968	0.371	0.988	0.3705	0.020	0.0005
0.032	0.871	0.012	0.8705	0.020	0.0005
0.468	0.9414	0.461	0.9409	0.007	0.0005
0.995	0.4982	0.000	0.500	0.005	0.0018
0.505	0.3142	0.505	0.3159	0.000	0.0017
0.495	0.8142	0.495	0.8159	0.000	0.0017
0.005	0.9982	0.000	0.000	0.005	0.0018
0.457	0.5608	0.461	0.5591	0.004	0.0017
0.043	0.2516	0.047	0.250	0.004	0.0016
0.957	0.7516	0.953	0.750	0.004	0.0016
0.543	0.0608	0.539	0.0591	0.006	0.0017
0.995	0.6289	0.012	0.6295	0.017	0.0006
0.505	0.1835	0.505	0.1841	0.000	0.0014
0.005	0.1285	0.988	0.1295	0.017	0.001
0.495	0.6835	0.495	0.6841	0.000	0.0006

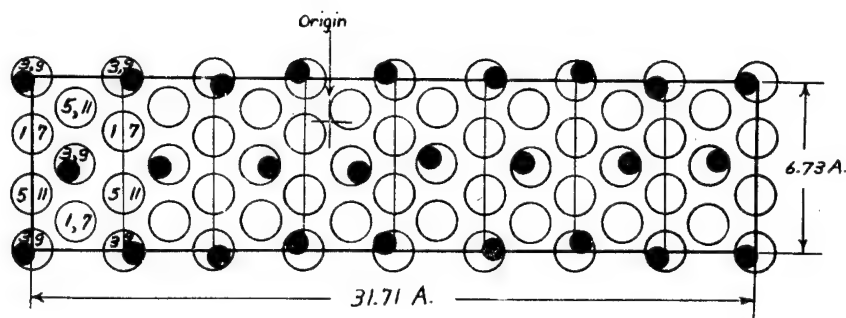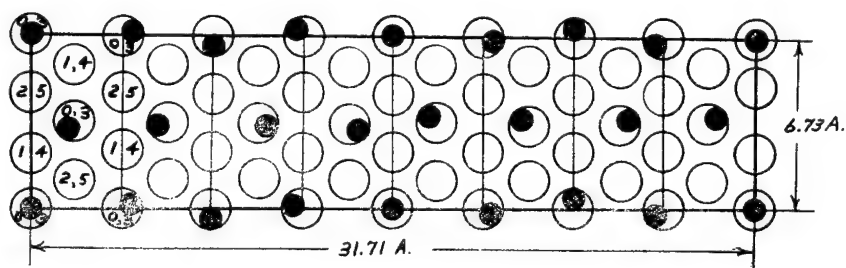*0.250 has been added to the x and 0.4062 has been added to the y coordinates.

Fig. 7--Projection of the U_2O_5 structure on (001)--A arrangement. (The solid circles are uranium atoms; the open circles are oxygen atoms as in UO_3. The numbers refer to the $\underline{z}$ coordinates in twelfths.)

Fig. 8--Projection of the U_2O_5 structure on (001)--C arrangement. (The solid circles are uranium atoms; the open circles are oxygen atoms as in UO_3. The numbers refer to the $\underline{z}$ coordinates in sixths.)

Table 19

Intensity Comparisons for U_2O_5: (0kℓ) Data

| Indices | Calculated | | Observed |
	Positions A	Positions C	
020	0	0	0
040	0	0	0
060	70	90	150
080	0	0	0
0,10,0	210	220	280
0,12,0	6	2	0
0,14,0	2	2	0
0,16,0	7950	7980	3450
0,18,0	6	3	0
0,20,0	0	6	0
0,22,0	360	450	390
0,24,0	0	1	0
0,26,0	440	480	430
0,28,0	24	16	0
C,30,0	3	5	0
0,32,0	2400	2440	2070
0,34,0	8	7	0
0,36,0	6	39	0
0,38,0	760	1150	650
0,40,0	0	19	0
021	0	0	0
041	0	1	0
061	6	15	0
081	0	1	0
0,10,1	2	5	0
0,12,1	0	0	0
0,14,1	0	0	0
0,16,1	1	3	12

Table 19

(Continued)

Indices	Calculated		Observed
	Positions A	Positions C	
0,18,1	0	0	0
0,20,1	0	0	0
0,22,1	5	20	19
0,24,1	0	0	0
0,26,1	4	9	19
0,28,1	0	1	6
0,30,1	0	2	5
0,32,1	3	2	170
0,34,1	0	0	0
0,36,1	1	1	50
0,38,1	2	20	390
0,40,1	0	2	0
022	0	0	0
042	0	0	0
062	2	15	0
082	0	0	0
0,10,2	30	37	0
0,12,2	1	0	0
0,14,2	0	0	0
0,16,2	650	640	430
0,18,2	2	0	0
0,20,2	1	1	0
0,22,2	220	260	230
0,24,2	0	0	0
0,26,2	320	390	430
0,28,2	24	6	0
0,30,2	3	4	0

Table 19

(Continued)

Indices	Calculated		Observed
	Positions A	Positions C	
0,32,2	2060	2140	2300
0,34,2	11	5	0
0,36,2	7	29	0
0,38,2	790	1180	650
0,40,2	0	12	0
023	0	3	0
043	0	0	0
065	20	53	0
083	1	3	0
0,10,3	4	32	0
0,12,3	0	1	0
0,14,3	0	1	0
0,16,3	1	3	0
0,18,3	0	0	0
0,20,3	1	1	0
0,22,3	21	68	120
0,24,3	1	4	0
0,26,3	27	49	130
0,28,3	2	10	50
0,30,3	1	10	40
0,32,3	26	15	170
0,34,3	0	5	0
0,36,3	7	12	70
0,38,3	35	256	390
024	0	1	0
044	0	0	0
064	6	4	0

Table 19

(Continued)

Indices	Calculated		Observed
	Positions A	Positions C	
084	0	0	0
0,10,4	13	20	0
0,12,4	0	0	0
0,14,4	0	0	0
0,16,4	440	440	500
0,18,4	0	0	0
0,20,4	0	0	0
0,22,4	60	60	150
0,24,4	0	0	0
0,26,4	190	270	430
0,28,4	20	0	0
0,30,4	4	0	0
0,32,4	2070	1990	2300
0,34,4	8	1	0
0,36,4	10	21	0
025	1	3	0
045	0	0	0
065	55	110	0
085	2	5	0
0,10,5	2	47	0
0,12,5	0	0	0
0,14,5	2	1	0
0,16,5	2	4	0
0,18,5	0	4	0
0,20,5	1	0	0
0,22,5	19	65	50
0,24,5	2	5	0

Table 19

(Continued)

Indices	Calculated		Observed
	Positions A	Positions C	
0,26,5	60	98	120
0,28,5	4	22	40
0,30,5	4	25	30
0,32,5	80	35	200
0,34,5	20	13	0
026	0	3	0
046	0	9	0
066	6	0	0
086	0	4	0
0,10,6	13	35	0
0,12,6	2	5	0
0,14,6	0	2	0
0,16,6	450	400	430
0,18,6	0	0	0
0,20,6	0	1	0
0,22,6	56	46	100
0,24,6	0	4	0
0,26,6	170	325	350
0,28,6	31	4	0
0,30,6	8	23	0
0,32,6	3390	3210	2500
027	1	2	0
047	0	2	0
067	69	140	0
087	2	6	0
0,10,7	49	101	0

Table 19

(Continued)

Indices	Calculated		Observed
	Positions A	Positions C	
0,12,7	0	1	0
0,14,7	70	3	0
0,16,7	8	74	0
0,18,7	1	1	0
0,20,7	2	9	0
0,22,7	80	250	80
0,24,7	6	11	0
0,26,7	160	270	120
0,28,7	14	64	80
028	0	5	0
048	2	19	0
068	4	0	0
088	0	10	0
0,10,8	10	48	40
0,12,8	4	16	0
0,14,8	2	6	0
0,16,8	660	500	500
0,18,8	0	4	0
0,20,8	2	22	0
0,22,8	130	109	190
0,24,8	0	32	0
0,26,8	510	1300	500
002	4890	4580	2300
004	2770	2660	1600
006	1360	1200	1000
008	810	630	900
0,0,10	1060	—	1200

The calculated intensities of the $(0.28, \ell)$ and $(0.36, \ell)$ reflections may be improved by changing the y parameters 0.1546 to 0.154 and 0.2227 to 0.222. Certainly, a major portion of the discrepancies between the calculated and observed intensities which remain could be due to the approximate absorption correction. Projections of the arrangements on the (y, z) plane are shown in figures 9 and 10.

The intensities of the diffraction maxima which are observed indicate strongly that the uranium atoms are only slightly removed from their original positions in the UO_3 structure. If one also assumes that a few oxygen atoms have been removed, that the remaining oxygen atoms have moved slightly from their positions in UO_3, and that the positions describing the oxygen positions in U_2O_5 could also describe them (with different parameters) in UO_3, then, space groups of much lower symmetry must be chosen. The UO_3 structure does not possess a mirror plane perpendicular to the unique axis. If one arbitrarily chooses a unit cell of the size and shape of U_2O_5 in the UO_3 structure, then the symmetry of this unit cell is much lower than the hexagonal symmetry of the simplest UO_3 unit cell. This larger unit cell, possesses only one two-fold axis with a mirror or glide plane normal to the two-fold axis. The highest possible space group which can describe both the uranium and oxygen atom positions is C_{2h}^2.

By an appropriate choice of parameters for the positions in space group C_{2h}^2, it is possible to place the uranium atoms in exactly the same positions as in space group D_{2h}^5. In addition, the ideal positions of oxygen atoms may be described in sets of four-fold positions. Of course, the uranium atoms could be placed in positions of lower symmetry in this space group, but there has been no apparent evidence requiring this possibility. Furthermore, uranium positions in the D_2 and C_{2v} space groups have not been considered since those in D_{2h}^5 appear to be satisfactory.

<div align="center">The Structure of U_3O_8</div>

X-ray data

Powder diagrams of U_3O_8 were taken on the unsymmetrical self-focussing powder camera. Its high dispersion enabled the complex diagrams to be resolved and the true unit cell described previously to be determined.

The intensities of the diffraction maxima were measured using an Eastman visual densitometer. The intensity measurements were complicated by the fact that the $K\alpha_1$, and $K\alpha_2$ separations were large enough that maxima from different planes overlapped. It was also difficult to obtain true background readings since some of the weak reflections caused the background to vary. The calculated intensities were found by the formula

$$I \propto FF*M.$$

Since many of the factors depending on Θ have been omitted, only adjacent reflections should be compared.

Structure determination

All the reflections which appeared on the powder diagrams could be indexed using an end-centered orthorhombic cell as described previously. No other general extinctions were observed. A restriction on the end-centered orthorhombic space groups is made, however, by requiring six uranium positions in the unit cell. As a result, only four orthorhombic space groups have the requisite positions. These space groups and their two-and four-fold positions are listed in table 20.

Since the pseudo unit cell has been expanded along the b direction, it is reasonable to expect a y parameter in the positions for the uranium atoms. This appears to be verified by the intensity data. Moreover, the intensity data seem to require a parameter in the x direction. For this reason it was necessary to use the positions in space group C_{2v}^{14}. The intensities were calculated for uranium atoms in the following positions:

(add 000, $\frac{1}{2}\frac{1}{2}0$ to all positions)

2 U at x' 0 0

4 U at x y 0   x $\bar{y}$ 0 .

The structure factor, F^2, for these positions is

$$f_U^2 \left[1 + 4 \cos 2\pi h(x' - x)\cos 2\pi ky + 4 \cos^2 2\pi ky \right].$$

This factor was evaluated for values of x' - x of 0.00, 0.02, and 0.04 and for the y values of 0.30, 0.31, 0.32, 0.333, 0.347, 0.357, and 0.367 for all the possible reflections. From this it appeared that suitable values of the parameters were x' - x = 0.04, y = 0.326. The intensities calculated on this basis are compared with the observed values in table 21. The agreement between adjacent reflections appears to be good. A projection of the U_3O_8 structure on the (x,y) plane is shown in figure 11.
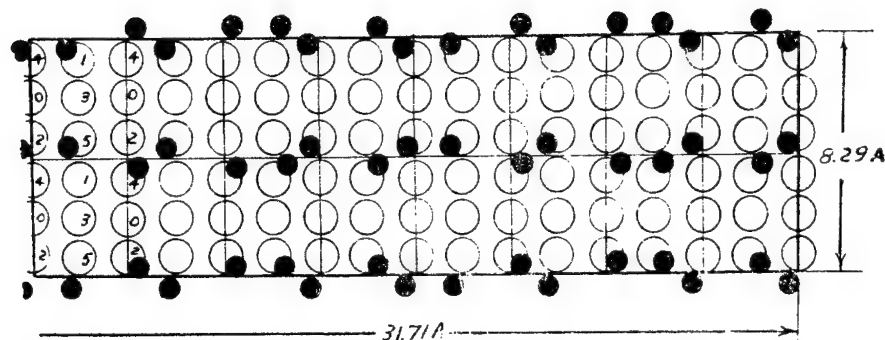
Fig. 9--Projection of the U_2O_5 structure on (100)--D_{2h}^{16} arrangement. (The solid circles are uranium atoms; the open circles are oxygen atoms as in UO_3. The numbers refer to the x coordinates in sixths.)
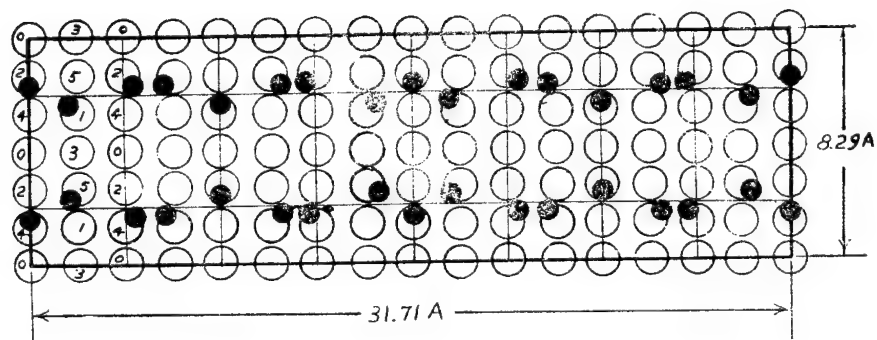

Fig. 10--Projection of the U_2O_5 structure on (100)--D_{2h}^{5} arrangement. (The solid circles are uranium atoms; the open circles are oxygen atoms as in UO_3. The numbers refer to the x coordinates in sixths.)

Table 20

Possible Uranium Positions for U_3O_8

Space group				Positions
				(add 000, $\frac{1}{2}\frac{1}{2}0$ to all positions)
D_{2h}^{19}	2 (a)	000	4 (g)	x00; $\bar{x}$00;
	2 (b)	$\frac{1}{2}$00	4 (h)	x0$\frac{1}{2}$; $\bar{x}$0$\frac{1}{2}$;
	2 (c)	$\frac{1}{2}$0$\frac{1}{2}$	4 (i)	0y0; 0$\bar{y}$0;
	2 (d)	00$\frac{1}{2}$	4 (j)	0y$\frac{1}{2}$; 0$\bar{y}\frac{1}{2}$;
			4 (k)	00z; 00$\bar{z}$;
			4 (l)	0$\frac{1}{2}$z; 0$\frac{1}{2}\bar{z}$;
D_2^6	Has same two- and four-fold positions as D_{2h}^{19}.			
C_{2v}^{14}	2 (a)	x00	4 (c)	x0z; x0$\bar{z}$;
	2 (b)	x0$\frac{1}{2}$	4 (d)	xy0; x$\bar{y}$0;
			4 (e)	xy$\frac{1}{2}$; x$\bar{y}\frac{1}{2}$;
C_{2v}^{11}	2 (a)	00z	4 (d)	x0z; $\bar{x}$0z;
	2 (b)	0$\frac{1}{2}$z	4 (e)	0yz; 0$\bar{y}$z;

Table 21

Intensity Comparisons for U_3O_8

Indices	$Sin^2 \theta$ (x 10^4)		Intensities	
	Calculated	Observed	Calculated (F^2M)	Observed
150	1170	1173	45	45
240	1191	1192	57	45
310	1228	1226	103	90
002	1381	1380	900	860
060	1495 ⎤		840 ⎤	
151	1515 ⎦	1493	86 ⎦	600
241	1536		9	
022	1547		5	
112	1555 ⎤		25 ⎤	
330	1561 ⎦	1556	1530 ⎦	810
311	1574	1591	190	120
061	1840	1840	1570	720
132	1887	1885	3220	1190
331	1906 ⎤		2870 ⎤	
202	1908 ⎦	1907	1560 ⎦	1350
260	2022	2020	1420	700
042	2045		20	
222	2074	2069	107	17
400	2110	2102	614	310
170	2166	2163	64	63
350	2225	2219	148	84
420	2276	2268	184	91
261	2367	2365	2650	810
401	2455	2452	1140	430
171	2511	2510	122	39
152	2551 ⎤		70 ⎤	
242	2572 ⎥	2566	89 ⎥	170
351	2570 ⎦		282 ⎦	

Table 21

(Continued)

Indices	$\sin^2 \theta$ (x 10^4)		Intensities	
	Calculated	Observed	Calculated (F^2M)	Observed
312	2610⎤	2610	160⎤	200
421	2621⎦		347⎦	
080	2657		24	
440	2774	2764	113	13
062	2876	2875	1300	430
332	2942	2939	2370	640
081	3002		47	
003	3108⎤		666⎤	
441	3119⎦	3110	216⎦	220
280	3184	3180	77	24
370	3221	3214	83	24
023	3274⎤	3275	4⎤	24
113	3282⎦		18⎦	
510	3339	3329	184	44
262	3403	3406	2360	710
402	3491⎤	3493	1000⎤	590
190	3495⎦		1110⎦	
281	3529⎤		146⎤	
172	3547⎥	3547	106⎥	
371	3566⎦		162⎦	11
460	3605⎤		947⎤	
352	3606⎥	3614	246⎥	540
133	3614⎥		2450⎥	
203	3635⎦		1190⎦	
422	3657⎤		307⎤	
530	3671⎥	3666	836⎥	300
511	3684⎦		347⎦	
043	3772		15	
223	3801		85	

Table 21

(Continued)

Indices	Sin^2 θ (x 10^4)		Intensities	
	Calculated	Observed	Calculated (F^{2}M)	Observed
191	3840	3842	2080	310
461	3950	3949	1790	270
531	4016	4013	1620	300
082	4138		41	
0,10,0	4152 ⎤		57 ⎤	
442	4155 ⎦	4146	187 ⎦	10
153	4278		56	
243	4299		71	
313	4337 ⎤		129 ⎤	
550	4335 ⎦	4327	252 ⎦	30
0,10,1	4497		107	
390	4550	4548	870	160
282	4565		125	
372	4602 ⎤		138 ⎤	
063	4603 ⎦	4605	1030 ⎦	230
333	4669 ⎤		1874 ⎤	
2,10,0	4679 ⎥	4670	95 ⎥	410
551	4680 ⎦		487 ⎦	
512	4720 ⎤		306 ⎤	
600	4747 ⎥	4742	315 ⎥	90
480	4767 ⎦		198 ⎦	
192	4876 ⎤		1830 ⎤	
391	4895 ⎦	4874	1630 ⎦	440
620	4913		254	
462	4986	4985	1570	170
2,10,1	5024		184	
532	5052	5054	1430	260
601	5092		609	

Table 21

(Continued)

Indices	Sin^2 θ (x 10^4)		Intensities	
	Calculated	Observed	Calculated (F^{2}M)	Observed
481	5112		383	
263	5130	5132	1890	240
1,11,0	5156		69	
403	5218	5220	800	130
621	5258 ⎤		490 ⎤	
173	5274 ⎦	5272	85 ⎦	60
570	5331		102	
353	5333	5324	197	20
423	5384	5384	246	10
640	5411		152	
1,11,1	5501		115	
0,10,2	5533 ⎤		97 ⎤	
004	5525 ⎦	5528	486 ⎦	110
571	5676	5678	197	10
024	5691		3	
114	5699		14	
552	5716	5716	438	80
641	5756		294	
083	5765		32	
443	5882		152	
392	5931	5934	1460	130
0,12,0	5979	5971	380	10
134	6031	6031	1620	250
204	6052 ⎤		880 ⎤	
2,10,2	6060 ⎦	6062	165 ⎦	90
602	6128 ⎤		546 ⎤	
482	6148 ⎦	6132	343 ⎦	70
044	6189		12	

Table 21

(Continued)

Indices	Sin² θ (x 10⁴) Calculated	Observed	Intensities Calculated (F²M)	Observed
3,11,0	6211		150	
224	6218		65	
660	6242	6239	514	40
4,10,0	6262		92	
283	6292⎤	6291	109⎤	60
622	6294⎦		456⎦	
0,12,1	6324⎤	6325	760⎤	110
373	6329⎦		120⎦	
513	6447	6444	255	20
710	6503⎤	6506	219⎤	160
2,12,0	6506⎦		688⎦	
1,11,2	6537		123	
3,11,1	6556		288	
661	6587	6588	988	150
193	6603⎤	6613	1600⎤	120
4,10,1	6607⎦		176⎦	
590	6660		94	
154	6695		44	
572	6712⎤		182⎤	
463	6713⎥	6713	1350⎥	90
244	6716⎦		55⎦	
314	6754		101	
533	6779	6780	1230	120
642	6792		272	
730	6835⎤		418⎤	
711	6848⎥	6852	438⎥	100
2,12,1	6851⎦		1280⎦	

Table 21

(Continued)

Indices	Sin^2 θ (x 10^4)		Intensities	
	Calculated	Observed	Calculated (F^{2}M)	Observed
591	7005	6994	1050	100
064	7020	7026	821	80
334	7086	7088	1500	180
1,13,0	7149		70	
731	7179	7176	800	90
0,10,3	7260	7262	83	10
0,12,2	7360	7363	700	60
680	7404		309	
553	7443	7441	390	30
1,13,1	7494⎤	7495	140⎤	40
750	7499⎦		325⎦	
264	7547	7550	1550	200
3,11,2	7592		277	
662	7623⎤	7625	910⎤	140
404	7635⎦		657⎦	
4,10,2	7643		162	
393	7658	7661	1290	140
174	7691		70	
681	7749⎤	7750	592⎤	30
354	7750⎦		161⎦	
2,10,3	7787		142	
424	7801		202	
751	7844⎤	7844	624⎤	100
603	7855⎦		483⎦	
483	7875⎤		303⎤	
712	7884⎥	7885	403⎥	140
2,12,2	7887⎦		1270⎦	
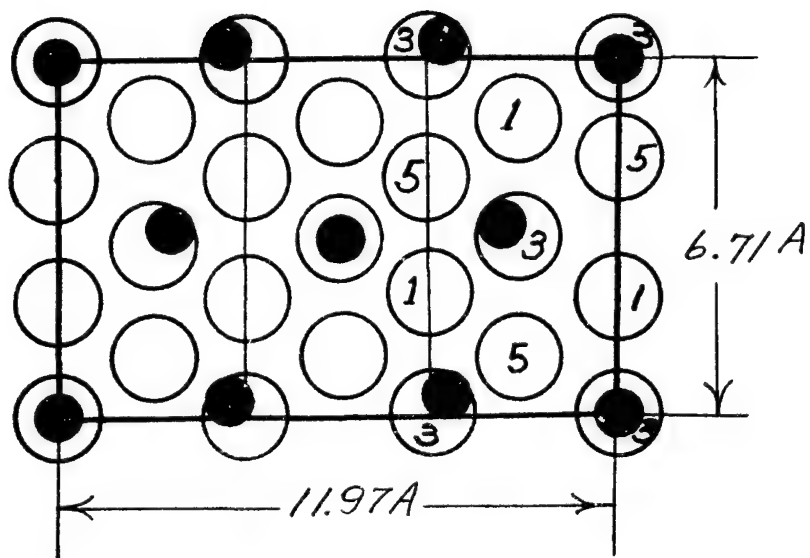
Fig. 11--The projection of the U_3O_8 structure on (001). (The solid circles are uranium atoms; the open circles are oxygen atoms as in UO_3. The numbers refer to the z coordinates in sixths.)

Again, as in U_2O_5, it is necessary to rely on a monoclinic space group to place the oxygen atoms if they are to have positions almost identical to those in UO_3. Either space group C_{2h}^3 or C_2^3 is possible; the latter is preferable, since it provides identical uranium positions to those in C_{2v}^{14}.

Discussion of the Structures

The relation between U_2O_5 and U_3O_8

A possible relationship between the U_2O_5 and U_3O_8 unit cells was observed as the result of single crystal rotation diagrams taken with the axis of rotation normal to the needle axis. If the axis of rotation is normal to the plane (130), then, the rotation diagram has a complex system of layer lines. The layer lines, 0, 16, and 32 are observed strong; the layer lines 1, 5, 6, 10, 11, 15, 17, 21, 22, 26, 27, 31, and 33 are weak. Thus, at first glance it would appear that the unit cell dimension of the UO_3 pseudo cell was only tripled. Since the unit cell found for U_3O_8 appears to have one pseudo cell dimension tripled, it is probable that the U_3O_8 unit cell is chosen at a rotation of 60° from the U_2O_5 unit. This relationship is indicated in figure 12.

The oxygen positions

The oxygen positions in the U_3O_8 and U_2O_5 structures can be determined only by inference from the shift of the uranium atoms. This is a difficult task, and the results cannot be upheld with much confidence. The relationship between the unit cells of U_3O_8 and U_2O_5 would indicate that for each oxygen vacancy in U_3O_8 there would be two in U_2O_5 above one another in the c direction. In addition, other oxygen atoms must be removed producing the shift in uranium atom positions which requires the larger unit cell. Therefore, it would be appropriate to consider U_3O_8 first.

The UO_3 oxygen positions in the U_3O_8 unit cell may be described on the basis of the monoclinic space group, C_2^3. In order to achieve the composition U_3O_8, two oxygen atoms must disappear. The only two-fold positions for oxygen atoms which can be removed are the uranyl oxygen atom positions along the c axis between the uranium atoms located at

the corners and center of the unit cell. Their removal would leave the structure with two uranyl uraniums to one uranous uranium atom.

Apparently, these same oxygen vacancies do not remain in the U_2O_5 structure. At least, there does not appear to be a relationship between the shift in uranium positions in this structure to that in U_3O_8. The $\underline{z}$ parameters for the uranium atoms at $y = 0$, $1/4$, $1/2$, and $3/4$, have shifted to such an extent that apparently one of the uranyl oxygen atoms must be missing at each of these positions. It is possible that one uranyl type oxygen atom is also missing at $y = 3/16$, $5/16$, $11/16$, and $13/16$. The other oxygen atom vacancies are not as easily determined. Also, it is not clear whether a total of sixteen oxygen atoms are missing as would be required for U_2O_5.

Summary and Conclusions

1. The positions of the uranium atoms have been found for the phases, U_2O_5 and U_3O_8. The positions are listed below.

For U_2O_5, space group D_{2h}^5

8U at x,y,z; $\bar{x},\bar{y},\bar{z}$; $x,\frac{1}{2} - y,z$; $\bar{x},\frac{1}{2} + y,z$;

$x,y,\bar{z}$; $\bar{x},\bar{y},z$; $x,\frac{1}{2} - y,\bar{z}$; $\bar{x},\frac{1}{2} + y,z$;

with $x = 0.539$, $y = 0.0591$, $z = 0.259$

8U at the same positions with $x = 0.988$, $y = 0.1295$, $z = 0.244$

8U at the same positions with $x = 0.505$, $y = 0.1841$, $z = 0.238$

4U at $x,\frac{1}{4},z$; $x,\frac{1}{4},\bar{z}$; $\bar{x},3/4,\bar{z}$; $\bar{x},3/4,z$;
with $x = 0.047$, $z = 0.265$

4U at $00z$; $00\bar{z}$; $0\frac{1}{2}z$; $0\frac{1}{2}\bar{z}$;
with $z = 0.220$

For U_3O_8, space group C_{2v}^{14} (add $000,\frac{1}{2}\frac{1}{2}0$ to all positions)
2U at $x00$ with $x = 0$

4U at $xy0$; $x\bar{y}0$ with $x = 0.04$, $y = 0.326$.

2. The relationship of the two structures to UO_3 is discussed.
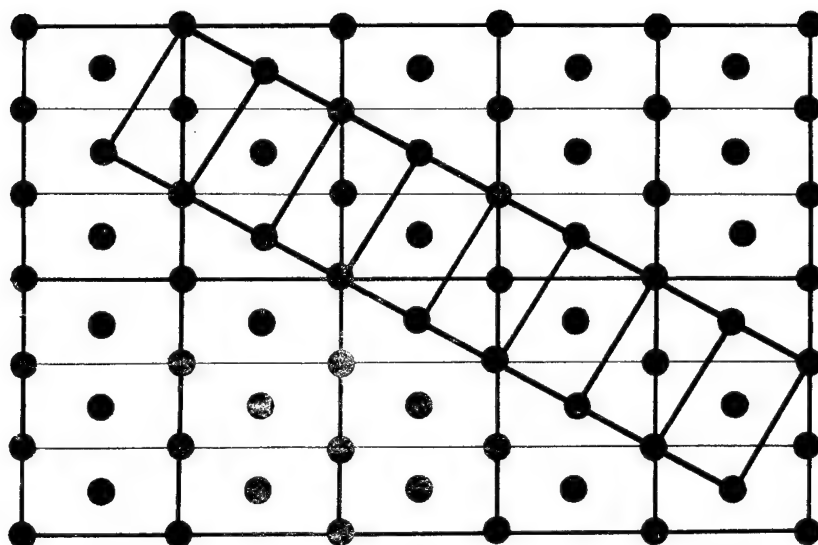
Fig. 12--The relationship between the unit cells of U_3O_8 and U_2O_5.

A NEW METHOD FOR THE DETERMINATION OF X-RAY INTENSITIES

Review of the Methods of Intensity Determination

An excellent review of the various methods of intensity determination in X-ray diffraction up to 1937 has been given by Halla and Mark (30). A more recent critical review of the photographic methods has been made by Robertson (31,32). The material in these reviews will be briefly summarized here and the more recent material added.

Ionization methods

Ionization chamber. The method which up to the present has provided the most accurate determination of intensities has been the measurement of the ionization of gases by X-rays using an ionization chamber. Applied to the determination of the intensity of reflections from single crystals, the instrument has taken the form of the ionization spectrograph. The method, although accurate to about 1 per cent, has required bulky equipment and a great deal of time to perform the measurements.

The Geiger-Müller counter. A more recent development has been the use of the Geiger-Müller counting tube to count the number of photons in the X-ray beam. The method has similar accuracy to that of the ionization chamber method, and it has been satisfactorily applied to the measurement of the intensities of powder haloes. It has not been any more satisfactorily applied to the measurement of single crystal diffraction maxima.

The electron multiplier tube. A quite new method involving the use of the electron multiplier tube (33,34,35) has been developed. The photoelectrons from the interaction of X-rays and a photoemissive metal provided the source of electrons which were multiplied to a measurable quantity in the same tube. Again, this method compares favorably with the earlier ionization and Geiger-Müller methods, but it has been just as difficult to apply to the measurement of single crystal diffraction maxima.

Measurement by photographic film

The most useful instrument for recording the intensities has been the photographic film. The record of a large number of reflections can be made rapidly and permanently. A large variety of methods have been developed for the determination of the intensities from the photographic film. All these methods must rely on the characteristic response of the photographic film to X-rays.

Film characteristics. It was shown by Bouwers (36) that the darkening, S, is proportional to It^P, where I is the intensity; t, the time of exposure; and p, the Schwarzschild exponent. Bouwers found that the value of p was 0.99 ± 0.02 or very nearly one. This has been more recently confirmed by Milbach (37) and Bell (38). The form of all the darkening versus the logarithm of exposure curves was explained by the relation

$$S = C \log (It/\gamma + 1),$$

where C and γ are constants depending on the developing time, temperature, and the wave length of the X-rays. For short exposures it was found that the blackening was directly proportional to the exposure, i.e., the first term in the expansion of $\log (It/\gamma + 1)$ or CIt/γ. Bouwers found that this region extended up to an optical density of 0.8. Other investigators found that the region occasionally extended up to 1 or 1.4 (39,40,41,42).

In more recent measurements by Bell (38) it was found that for single-coated film the density versus exposure curve was linear up to an optical density of 0.7 to 1 depending upon the film type. The density versus log exposure curve was linear from a density of 3 to 4 or 4.5 where solarization began. For double-coated film, however, the linear density-exposure range extended up to an optical density of 2. The extent of the linear region depended solely on the film type and the type of developer. Double-coated non-screen X-ray film of the type commonly used in X-ray diffraction work was found to have the greatest range of linearity.

The blackening of photographic film by X-rays is independent of wave length for a large range of the X-ray spectrum. The most notable variance found by early workers was at the wave lengths corresponding to the silver and bromine absorption edges. More recently, Milbach (37) has investigated the effect of long wave length X-rays and has found that the form of the density versus exposure curve approached that of

visible light as the wave length became longer. The change did not become pronounced until wave lengths greater than 4 A. were used.

Visual estimation of blackening. The visual method has been used more extensively than any other method for estimating intensities for structure determination. In general, four methods have been used to establish a scale for numerical intensity estimates. (a). The ratio of the intensities of the $K\alpha_1$, $K\alpha_2$ and $K\beta$, lines, which is accurately known as 100::50::17, has provided one scale. (b). The multiple film method, which depends on the fact that a single sheet of X-ray film absorbs a constant fraction of the original beam has provided another scale. In this method the films are placed in back of one another with respect to the X-ray beam, exposed and developed simultaneously. The intensities of the spots on succeeding films removed from the X-ray beam are proportional to decreasing powers of the absorption factor. (c). The maxima on the film have been compared with standard spots printed on the same film using a sectored X-ray beam or they have been compared with spots on a diagram of a crystal whose structure was known. (d). In the internal standard method the maxima of a standard crystal of known structure have been recorded on the same film for comparison.

Although the accuracy varied with the care of estimation and the type of numerical scale which was used, intensities were judged with an error of 20 per cent. Some investigators (30) have claimed an error of only 9 per cent. The intensities obtained as an average of several independent judgments have been usually sufficient to determine the positions of the atoms with an error of 0.01 to 0.02 A. Confidence in the judged values of intensities, however, is gained only through experience, and the mental anguish of many decisions has spurred the search for a more impartial method of estimation.

Photographic printing methods. Several methods have been developed which relieve the tedium of judging but do not greatly improve the accuracy. Meisel (43) by means of a slit camera, converted the maxima from the shape of a curved line or spot into straight lines of even density several centimeters long. This positive was then printed through a gray wedge. The lines appeared on the print as narrow peaks. The heights of the peaks above the background were proportional to the intensities.

Lukesh (44) made a series of exposures of varying time on to high contrast printing paper. The printing time necessary to produce darkening

in the white center of the spot or line on the print was proportional to the intensity.

Astbury (45,46,47) developed a method of integrating the intensity of a spot. The bichromated gelatin process which he applied produced a thickness of film which decreased with increasing density. By measuring the number of alpha particles from a constant source which penetrated the film, he was able to measure the integrated intensity of the spot. The process had to be very closely controlled to produce reliable intensities.

Quite recently Dawton (48) has developed a positive film photometer. A print of the X-ray negative was made on a commercial process film so chosen that the transmittancy versus X-ray exposure curve was linear. The transmittancy of the whole spot was then measured photoelectrically. The method was reported to be accurate to within 1 per cent for weak reflections, within 5 per cent for medium spots and within much wider limits for the more intense spots where the deviation from linearity became more important. The method was rapid and convenient once the film and printing process were carefully selected.

Optical density measurements. Since the relationship of blackening to exposure is known, a measurement of the optical density suffices to determine the intensity. If I_0 is the intensity of the incident light beam; I, the intensity of the transmitted light beam, log I_0/I is equal to the optical density or blackening of the film. The measurement of the light intensity is performed conveniently by a photocell. The microphotometer has been used for the measurement of the intensity of Debye-Scherrer lines. This instrument measures and records the optical density at each point across a line. The area under the peaks in the density-position curve is proportional to the intensity. If necessary, corrections can be applied for the non-linearity of the density-exposure curve.

The problem of measuring a spot produced by diffraction from a single crystal was not as easily solved. The time required to make a large number of microphotometer traces over a spot and to calculate the intensity from the data was too large to be profitable. Robinson (49,50) produced an ingenious photometer which balanced the density at each point against a gray wedge printed on the same film. The density was balanced at 300 points spaced 0.1 mm. apart in a grid over the reflection. The movements of the gray wedge were mechanically integrated to give a value of the integrated intensity. After the spot had been

properly aligned, the measurement required only five or ten minutes. The accuracy of this method (about 1 per cent) compared with that of the ionization chamber method over the whole range of intensities.

Dawton (32) applied modern television equipment in his scan photometer to scan the spot in a fraction of a second. A non-linear circuit in the amplification stage was used to correct for the density-exposure curve. The integrated density measurement was read directly. The method was accurate to 1 per cent on weak and moderate intensities, but did not correct adequately for the large intensities.

Scattering method. The scattering of light by the grains of silver in the emulsion of a photographic film is proportional to the number of grains present. The number of silver grains in an X-ray film is proportional to the intensity over the lower range of densities. Brentano (51) used this principle to obtain integrated intensities of weak reflections. The method is extremely accurate for low densities of silver.

Measurement of Intensities by the Radioactive Toning Process

In this new method of determining intensities the photographic record of the diffraction pattern is toned with a radioactive solution. The intensities of the diffraction maxima are found by measuring the activities of the spots. The accuracy of the method depends upon several assumptions which must be tested.

(a) The number of silver atoms deposited on the photographic film must be directly proportional to the intensity of the X-ray beam causing the deposit.
(b) The toning process must deposit an activity which is proportional to the number of silver atoms.
(c) The activity must be determined accurately and rapidly.

There are indications that the first assumption is correct since it has been shown (52) that the weight of silver is proportional to the optical density. The optical density is proportional to the exposure up to optical densities of two. Still, the three assumptions are interrelated, and the counting rate versus exposure relationship must be investigated.

The choice of the toning process

The choice of the method of radioactive deposition depended on the following conditions:

   (a)   the deposition must be proportional to the number of silver atoms present in the negative;
   (b)   the activity must be easily measured;
   (c)   the solutions must be stable chemically;
   (d)   the solutions must be fairly stable in a radioactive sense, i. e., the half-life of the activity must not be too short.
   (e)   the radioactive isotope must be available;
   (f)   the specific activity of the radioactive isotope which is attainable must be sufficient to produce a measurable activity.

The neutron bombardment method. The first attempt to produce activity on the film did not involve a chemical process but a physical one. The method depended upon the neutron capture by the silver on the film to produce a silver isotope with a 225 day half life. Although calculations indicated that sufficient silver activity could be produced on the film, it was found that not only the film base disintegrated under the heavy neutron bombardment but also a very high background of a 15 day activity resulted which completely masked the silver activity.

Chemical toning methods. The common photographic toning processes (53,54) were the most obvious methods. The sepia toning processes deposit sulfur as Ag_2S. A radioisotope of sulfur is available, but the beta particle is easily absorbed, and the toning solutions are not particularly stable. The selenium toner is similar to the sepia toner in regard to stability and difficulty of getting the radioactive atom into the toning solution. The gold toner deposits gold, but a suitable radioisotope is lacking. The ferrocyanide toners offer a wide range of metal ferrocyanides which can be deposited on the film. Any of the insoluble ferrocyanides of iron, cobalt, nickel, lead, uranium, etc. are possible reagents. For most of these, satisfactory radioisotopes are lacking. However, Co^{60} is a striking exception. Its half-life is approximately five years; it emits several strong gamma rays (1.1 MEV and 1.3 MEV) and a moderately weak beta ray (0.31 MEV). It is also available in specific activities up to 100 millicuries per gram.
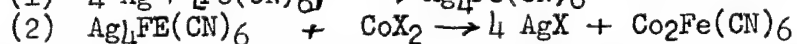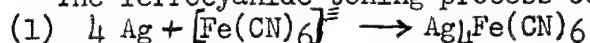
Chemical intensification methods. The mercury intensifier deposits Hg_2Cl_2 on the film in its initial step. The mercury isotope, Hg^{203} or 5, with a half life of 51.5 days and an available specific

activity of 11 millicuries per gram is another possible isotope. The chromium intensifier is unsuitable because of the radioactive nature of the chromium isotopes. The silver intensifier using the 225 day silver isotope may be suitable; however, the intensifying solutions are not particularly stable.

The chemistry of the cobalt toning process

The most promising of all the methods seemed to be the cobalt toning process. It fulfilled most of the requirements set out above. Thus, it is this method which has been investigated.

The ferrocyanide toning process consists of two steps.
(1) $4 \ Ag + [Fe(CN)_6]^{\equiv} \longrightarrow Ag_4Fe(CN)_6$
(2) $Ag_4FE(CN)_6 + CoX_2 \longrightarrow 4 \ AgX + Co_2Fe(CN)_6$
Mixed solutions which carry out both steps simultaneously have been reported (53,54,55,56,57), but they are unstable and decompose to form cobalt ferricyanide which does not react readily with the deposited silver. Solutions which carry out each step separately have also been reported. The toning solutions used by Hammarburg (58) are given below.

A	B
5 g $K_3Fe(CN)_6$	0.5 g Cobalt salt
100 ml H_2O	5 ml HCl
10 ml NH_4OH	100 ml H_2O

Strauss (57) has reported that small amounts of copper and nickel salts act as an accelerator to the cobalt toning process. Since nickel is the decay product of radioactive cobalt, the accelerator is auto- matically built into the solution.

In order to determine the important components and concentrations of the toning solutions, a series of qualitative tests were performed. In the first set of experiments, equal portions of $Ag_4Fe(CN)_6$ precipi- tate were treated with solutions which were 0.05 M. in cobaltous ion but in which the anion was varied. The results were determined visually by the amount of green precipitate of $Co_2Fe(CN)_6$ formed. Cobalt sulfate solutions did not react. With hydrochloric acid added to the cobalt sulfate solution, the extent of reaction increased with increasing hydrochloric acid concentration up to approximately 1 N. where the reaction appeared to be complete. Sodium chloride was substituted for the hydro- chloric acid with no apparent change in the extent of the reaction. Neutral solutions of cobaltous chloride also reacted completely.

These experiments indicate that it is the reaction between the silver ions in the silver ferrocyanide with the halogen ions of the toner to produce silver chloride which makes the reaction proceed rapidly. Bromides have been reported (54) to be more efficient toning agents in the ferrocyanide toning processes, evidently due to the greater insolubility of silver bromide. By a series of dilutions experiments it was found that solutions as low as 0.005 M of cobaltous chloride or cobaltous bromide would react satisfactorily with the silver ferrocyanide.

The action of the bleaching solutions, A, upon totally blackened film showed that the solutions bleached more rapidly as the ammonium hydroxide concentration was increased. The dissolution of the silver ferrocyanide was also increased.

Preparation of the radioactive toning solution.

The small pellets of metallic cobalt as supplied by the Oak Ridge National Laboratory were dissolved in nitric acid. The cobaltous nitrate solution was converted to cobaltous bromide by repeated evaporations with an excess of hydrobromic acid. The solution was finally evaporated to dryness on a steam bath. This material was then diluted with water to approximately 100 ml. This 100 ml. of solution contained 0.04 grams of cobalt and approximately 1.2 millicuries of activity. Earlier experiments with a diluted cobalt activity had shown that this activity was necessary to produce a sufficiently high counting rate. Larger activities become difficult to handle because of shielding problems.

Counting methods.

The activity from the spots was counted using a thin-walled (3 mg. per sq. cm.) Victoreen Geiger-Müller counting tube. The pulses were recorded by a standard scaling circuit and mechanical counter. The hard gamma ray which was present prevented counting the spots while still attached to a large area of film. The spots were punched from the film base using hand paper punches outfitted with dies in the shape of small circles and rectangles. The smallest circle and rectangle each had an area of approximately 0.018 cm.^{2} The next smallest circular and rectangular areas which could be obtained were 0.095 cm.^{2} The background was determined by punching out an area on the film adjacent to the single

crystal spot. The punchings were mounted on a lead disk on a counter shelf which could be placed at various horizontal levels beneath the counting tube window.

The geometry of the samples with respect to the counting tube window was very reproducible. In all tests which were made, the geometrical error was much less than the statistical error in counting. Even when the punchings were arbitrarily displaced several millimeters from their usual position, no change in the counting rate could be detected.

The counting error due to the "dead" time of the counting tube was corrected when necessary by the formula,

$$N/(1 - Nt) = N_{true},$$

where N_{true} is the true counting rate, N is the counting rate observed, and t is the dead time of the counter.

It would be desirable to be able to make an instantaneous reading of the activity of the spot. Since radioactive decay is statistical in nature, the accuracy depends on the total number of counts recorded. The time involved to make the measurement then depends directly on the accuracy desired and the intensity of the spot. In all cases, a minimum of 12,000 counts were recorded. This reduces the standard error to approximately 0.9 per cent of the total count.

Determination of the optimum toning procedure

Preparation of standard spots. A standard set of spots was prepared upon which to test the conditions of the toning process. The spots were formed by exposing film to an X-ray beam with a brass plate containing eight holes interposed between the film and the X-ray source. The film, contained in a black paper envelope, was placed tightly against the brass plate. The holes (0.04 in. in diameter) in the plate were spaced so that an eight step sector could produce a series of eight spots in which the intensities varied as 1, 2, 4, 8, 16, 32, 64, and 128. The sector, multiple pin-hole system and film-holder were placed five feet from the target of a self-rectifying gas type X-ray tube.

Calibration of the pin-hole system. Double-coated Eastman no-screen X-ray film was exposed to the unsectored beam to produce eight spots of approximately equal intensity. The film was developed in

Eastman Kodak X-ray developer, fixed in a solution prepared from East-man Kodak acid fixing powder, washed, and dried in the usual manner. Before toning, the dried film was soaked in water for one-half hour in order to improve the evenness of toning. The film was then bleached in a solution of five grams of $K_3Fe(CN)_6$, 100 ml. of water and ten drops of ammonium hydroxide for one hour, washed for one hour, toned in the radioactive cobalt bromide solution for two hours, placed for one hour in 100 ml. of distilled water to dilute the occluded activity, placed in two liters of water for one hour to further dilute the activity, and finally washed in running water for one hour and dried.

Each of the eight spots was carefully counted to determine the ratio of intensities of the spots.

Table 22

Ratio of Intensities of the Standard Spots

Spot no.	Experiment I	Experiment II
1	1.000	1.000
2	1.030	1.023
3	.987	.972
4	.984	.996
5	1.089	1.062
6	.996	.987
7	1.046	1.038
8	.939	.943

The results of two determinations, each an average of two counts of approximately 10,000 counts, is shown in table 22. These intensity ratios enabled the variance in the size of the holes in the brass plate and in the X-ray beam intensity to be corrected.

Determination of cobalt toning time. A series of films each re-
ceiving approximately the same exposure (optical density = 1.7) were
prepared. Two of the eight spots on each film were toned simultaneously
and served as control spots for the experiments. Since the ratio of
their intensity to the other spots was known from above, the inequality
of exposure from film to film could be corrected. The remaining six
spots, all given the same bleaching treatment as above, were toned for
periods of fifteen, thirty, and sixty minutes. It was found that at the
end of fifteen minutes the toning was 96 per cent completed and totally
completed at the end of thirty minutes. Thus, for any toning period over
a half hour there is no change in activity.

Determination of bleaching conditions. The bleaching solutions
were tested both for time of bleaching and the composition of the bleach
using the same method for control of the experiment as before. The films
were bleached in bleach X for 5, 10, 15, 30 and 60 minutes or in bleach
Y for 5, 10, 20, and 40 minutes. All films were toned in the cobalt
solution

Bleach X	Bleach Y
5 g $K_3Fe(CN)_6$	5 g $K_3Fe(CN)_6$
100 ml water	100 ml water
10 drops NH_4OH	10 ml NH_4OH

for 30 minutes. The bleaching action of X appeared to be complete at
the end of five minutes, and the activity of the spots did not vary for
bleaching times up to one hour. The bleaching action of Y was not only
complete at the end of five minutes, but it had reduced the background
counting rate due to chemical fog from 1300 counts per minute to 120
counts per minute. In addition, it removed 20 per cent of the silver
in the spot as indicated by the lower counting rate. At the end of forty
minutes 67 per cent of the silver in the spot had been removed. Thus,
the NH_4OH in bleach Y acts as a cutting reducer and bleach Y is un-
satisfactory unless used for a period less than five minutes. Even
then it would prove unsatisfactory since short bleaching times would in-
troduce errors due to unequal diffusion of chemicals in the gelatin.

The concentration of NH_4OH in the bleach was varied between X and
Y and tested on standard spots using five minute bleaching times. Con-
centrations of NH_4OH up to 1 ml. per 100 ml. of solution appeared to be
satisfactory.

Final chemical process. As a result of the experiments above, the following processing method has been adopted:

    (a) the X-ray films conventionally developed, fixed, washed, and dried, were soaked in water for 30 minutes;

    (b) bleached in bleach X for a minimum of 30 minutes;

    (c) washed in running water for one hour;

    (d) toned on cobalt toner for a minimum of 30 minutes;

    (e) the occluded activity diluted in 100 ml. of water for one hour, followed by further dilution in two liters of water for one hour;

    (f) finally, washed in running water for one hour and dried.

All the processing was carried out at 20° C. and in ordinary light except that the films were handled in subdued light during steps (b) and (c).

Counting rate vs. exposure curves

A linear relationship between the optical density and exposure which extends up to an optical density of two was found by Bell (38) for double-coated non-screen X-ray film. Sheppard and Ballard (52) showed that the mass of silver deposited on the film is proportional to the optical density. Since in the toning process cobalt is deposited proportional to the mass of silver present, the counting rate should be proportional to the exposure. The counting rate vs. exposure relationship has been determined for Eastman double-coated X-ray film.

A series of eight spots were prepared on Eastman film using the brass mask and eight step sector described previously. The films were toned using the final toning procedure described above. The spots were punched from the film and counted for two measurements of at least 10,000 counts each. The counting rates were corrected for the dead time of the counter, the background counting rate due to the chemical fog, and the relative size of the spots. The relationship among the counting rates and exposures is shown in table 23 for two separate experiments. The optical densities of the background and a few of the strongest spots were measured using an Eastman visual densitometer. These optical densities are listed in the table to indicate the densities of the spots.

Table 23

Counting Rate vs. Exposure Relationship

Exposure	Optical density	Counting rate (c/m ÷ 64)	Linear Response
Experiment I			
Background	0.10	10.05	
1		3.37	2.76
2		5.56	5.52
4		11.37	11.04
8		21.91	22.08
16		42.84	44.16
32	1.88	78.55	88.32
64	>3.	132.44	176.6
128	>3.	191.28	
Experiment II			
Background	0.10	9.76	
1		6.10	6.72
2		13.36	13.44
4		26.99	26.88
8	1.4	53.58	53.76
16	2.38	96.34	107.5

The optical density-exposure curve appears to be linear up to an optical density of 1.8 to 2.0. The deviation from the curve at low optical densities is due to the error introduced by subtracting a high background counting rate. The deviation at high optical densities is real, however, and amounts to approximately 10 per cent at an optical density of two. Agfa film was not tested because preliminary optical density measurements showed that the linear relationship did not extend nearly as far as for Eastman film.

Measurement of intensities of anthracene single crystals

It seemed desirable to test the intensity method further on a crystal whose intensities have been measured by other methods. The intensities of reflections from anthracene crystals have been measured by Robertson (59,31) and Robinson (60,49) by the ionization chamber and Robinson's photometer method. Banerjee (61) obtained the intensities by repeated microphotometering of the reflections. Therefore, multiple film Weissenberg and oscillation diagrams of anthracene crystals were prepared, and the intensities of the (00l) and (h0l) reflections were determined by the method outlined above.

The anthracene crystals, crystallized from acetone, were 0.2 mm. to 0.4 mm. in diameter. The spot area which was produced on the Weissenberg film was $\sim$0.001 cm? as compared to the smallest punching area of 0.018 cm? Each reflection was counted for at least 13,000 counts and corrected for the dead time of the counter and the background counting rate. The counting time per punching varied from three to ten minutes. The results of these determinations are compared with those of Robinson, Robertson, and Banerjee in table 24.

Evaluation of the method

Accuracy. Since the process of registering the original intensities of the X-rays is photographic, the method has all the inherent errors due to variable silver halide deposit, uneven development, losses due to solubility of the gelatin, etc. These errors may be reduced by careful regulation of the development process and by repetition of the experiments. Bell, however, (37) has concluded that the average error in any photographic density measurement is a variation of 1 per cent for measurements performed on the same film and 5 per cent for comparisons of measurements on different films.

Table 24

Intensities of Reflections from Anthracene Crystals

Indices	Ionization	Robinson's Photometer	Banerjee	Toning
200	1000	1000		1072
20$\bar{1}$	652	657		645
20$\bar{2}$	253	263		235
002	192	198	196	199
003	52	60	46	50
004	81	73	77	85
005	32	32	11	31

The second source of error is the non-linearity of the counting rate vs. exposure curve for large exposures. This error may be minimized by neglecting values from spots which appear to be totally opaque. Multiple films may be used to bring the spots into the correct exposure range. This, however, introduces the error due to the uncertainty of the film factor. This error should be much smaller than that due to non-linearity, however.

A third source of error lies in the bleaching and toning process. For films which are processed simultaneously, this should be minimized. The lack of stirring of the radioactive solutions is compensated by the long time of the processing.

A fourth source of error is due to that characteristic of the counting tube and circuit. The dead time can be measured and corrections made to less than 1 per cent. Variations in sensitivity due to light and due to counting tube voltage can be checked by counting a standard spot at regular intervals. The reproducibilty of the geometry of the samples with respect to the counting tube window has been shown to be very good, and errors due to this factor have not been detected.

A further source of error arises from the location of the crystal
in the X-ray beam. Errors of this type were noted in using large
anthracene crystals. The best agreement with the ionization method
was obtained over small translational distances on the Weissenberg
film (corresponding to a small rotation of the crystal). The widest
variation was obtained in comparing the (200) and the (20$\bar{2}$) reflections
which were separate by 50° on the film.

The above errors cannot be evaluated directly but can only be
indicated by the agreement of the results of this method with those
by other methods (see table 24). A fifth source of error, the statis-
tical error due to the measurement of the radioactive decay of the cobalt
can be estimated. The standard deviation for one measurement in which
$\underline{n}$ observations are made is equal to $\sqrt{\underline{n}}$. In a measurement of 10,000
counts the standard deviation is 1 per cent. Thus, the standard devia-
tion for one measurement can be easily lowered to less than one per
cent, and the measurement of the background counting rate can be de-
termined with similar accuracy. The counting rate of the spot, however,
is determined by the difference of the spot plus background counting
rate and the background counting rate. The standard deviation of the
resulting spot counting rate is equal to the sqare root of the sums
of the squares of the errors in each counting rate. Thus, if the
background counting rate is large compared to the spot counting rate,
the error in the latter may be very large. Only if the background
counting rate is zero, is the standard error in the spot counting rate
equal to the standard error of the measurement. Thus, the accuracy
of the method is primarily dependent on the importance of the back-
ground and the number of total counts which are recorded per spot.
Nevertheless, comparison of the values of intensity obtained by this
method with those found for the ionization chamber and Robinson's
photometer are good, even with rather high background errors.

Convenience. The method enjoys the convenience of simultaneous
registration of a large number of reflections on a photographic film.
It can be applied to any photographic record, obtained by any X-ray
diffraction method. The best diffraction method is one which produces
a low background and fairly large diffuse spots. The measurement of
the activity is a routine standard process which even non-technical
personnel can perform. The time of measurement for a spot with a con-
venient size varies from one to five minutes. Only very weak or ex-
tremely small spots require measurements of over ten minutes. The
equipment needed is standard equipment available in all modern lab-
oratories.

Possible improvements. Higher counting rates can be obtained by using cobalt with a larger specific activity. The cobalt used in these experiments had a specific activity of thirty millicuries per gram. Activities of 100 millicuries per gram are available.

The background error may be reduced by using smaller punches, or larger spots. The latter also increases the counting rate. The larger spots can be obtained by using larger crystals, larger camera radius, or by moving the film holder slightly during the exposure, thereby obtaining double spots or a broadened spot. Special film with a much heavier coating of silver halide which would extend the range of linearity would be desirable.

Summary and Conclusions

A new method of determining the intensities of X-ray diffraction maxima from their photograph record has been developed which involves the radioactive toning of the film. The method appears to be almost as accurate as the ionization chamber method. The measurement of the intensity of approximately 10 reflections can be determined per hour with an accuracy of less than 5 per cent.

LITERATURE CITED

1. Kaufmann, Caillity and Gordon, Manhatten Project Report, CT-1101 (1943)

2. Foote, Clark, Cieslicki, Nelson and Lane, Manhattan Project Report, CT-3013 (1945)

3. Carlson, To be published in Vol. 19, Division 5 of the National Nuclear Energy Series.

4. Noyce, ibid.

5. Rundle, Baenziger, Wilson and Snow, To be published in Acta Crystallographica.

6. Mehl and Mair, J. Am. Chem. Soc., 50, 55 (1928)

7. Hughes, J. Chem. Phys., 3, 1 (1935)

8. Bragg and Wood, J. Am. Chem. Soc., 69, 2919 (1947)

9. Lipson and Beevers, Proc. Phys. Soc. (London) 48, 772 (1936)

10. Bragg and Lipson, Z. Krist, 95, 323 (1936)

11. Hughes, J. Am. Chem. Soc., 63, 1737 (1941)

12. Jacob and Warren, ibid., 59, 2588 (1937)

13. Pauling, ibid., 69, 542 (1947)

14. Hume-Rothery, J. Inst. Metals, 35, 309 (1926)

15. Jones, Proc. Roy. Soc. (London), A144, 225 (1934)

16. Jones, ibid., A147, 396 (1934)

17. Pauling and Ewing, J. Am. Chem. Soc., 70, 1660 (1948)

18. Patterson, Z. Krist., 90, 517 (1935)

19. Goldschmidt and Thomassen, Videnskapsselskapets-Skrifter. I. M. nat. Klasse, Oslo, Nr. 2, (1923) /Original not seen; abstracted in Strukturbericht, 1, 212, 249 (1931)/

20. Van Arkel, Physica (Now Nederland. Tijdschr. Natuurkunde), 4, 286 (1924)

21. Schoep and Billiet, Bull. Soc. géol. Belg., 58, 198 (1935) /Original not seen; abstracted in Strukturbericht, 3, 302 (1937)/

22. Biltz and Müller, Z. anorg. allgem. Chem., 163, 257 (1927)

23. Lyden, Finska Kemistsamfundets Medd., 48, 124 (1939) /Original not seen; abstracted in C. A., 34, 4005 (1940)/

24. Pederagani and Rosenbaum, Manhattan Project Report, CP-1168 (1943)

25. Rundle, Baenziger, Wilson and McDonald, J. Am, Chem. Soc., 20, 99 (1948)

26. Zachariasen, Manhattan Project Report, CK-2667 (1945) Also to be published in Phys. Rev.

27. Grönvold, Nature, 162, 69, 70 (1948)

28. Jolibois, Compt. rend., 224, 1395 (1947)

29. "Internationale Tabellen zur Bestimmung von Kristallstrukturen", Rev. Ed., Band I, Gebrüder Borntraeger, Berlin, 1935.

30. Halla and Mark, "Leitfaden für die Röntgenographische Untersuchung von Kristallen", J. A. Barth, Leipzig, 1937, Reprinted by Edwards Bros., Ann Arbor, Michigan, (1944) pp. 239-264.

31. Robertson, J. Sci. Instruments, 20, 169 (1943)

32. Robertson and Dawton, J. Sci. Instruments, 18, 126 (1941)

33. Bay, Rev. Sci. Instruments, 12, 127 (1941)

34. Papp and Sasvari, _Muegyetemi Közlémenyek_, 1947, 171. [Original not seen; abstracted in _C. A._, 42, 2866 (1948)]

35. Allen, _Phys. Rev._, 59, 110 (1941)

36. Bouwers, _Z. Physik._ 14, 374 (1923)

37. Milbach, _Z. wiss. Phot._, 36, 269 (1937)

38. Bell, _Brit. J. Radiol._, 9, 578 (1936)

39. Friedrich and Koch, _Ann. Physik_, (Series 4), 45, 399 (1914)

40. Busse, _Z. Physik._, 34, 11 (1925)

41. Brindley and Spiers, _Phil. Mag._, 16, 686 (1933)

42. Glocker and Traub, _Physik. Z._, 22, 345 (1921)

43. Meisel, _Z. Krist._, 90, 92 (1935)

44. Lukesh, _J. Chem. Phys._, 9, 659 (1941)

45. Astbury, _Proc. Roy. Soc._, A115, 640 (1927)

46. Astbury, _Phot. J._, 68, 500 (1928)

47. Astbury, _Proc. Roy. Soc._, A123, 575 (1929)

48. Dawton, _Proc. Phys. Soc._ (London), 50, 919 (1938)

49. Robinson, _J. Sci. Instruments_, 10, 233 (1933)

50. Dawton, _J. Sci. Instruments_, 14, 198 (1937)

51. Brentano, _Phys. Rev._, 63, 64 (1943)

52. Sheppard and Ballard, _Phot. J._, 68, 354 (1928)

53. Neblette, "Photography, its Principles and Practice", 4th ed., Van Nostrand, New York, 1942, pp. 573-578, 644-661.

54. Clerc, "Photography; Theory and Practice", 2nd ed., Pitman, New York, 1940, pp. 378-389, 306-313.

55. Dureton, Bull. soc. franc. phot. (3), 6, 304 (1919)
    /Original not seen; abstracted in C. A., 14, 699 (1920)7

56. Nilsson, Brit. J. Phot., 86, 329 (1939)

57. Strauss, Phot. Ind., 1924, 282. /Original not seen; abstracted in
    in C. A., 19, 785 (1925)7

58. Hammarburg, Nord. Tid. Fot., 24, 184 (1940)
    /Original not seen; abstracted in C. A., 37, 2281 (1943)7

59. Robertson, Proc. Roy. Soc., A140, 79 (1933)

60. Robinson, Proc. Roy. Soc., A142, 422 (1934)

61. Banerjie, Indian J. Phys., 4, 557 (1930)

ACKNOWLEDGMENT

END OF DOCUMENT